New Concepts in Mass and Energy Transport using Graphene and Carbon Nanotubes

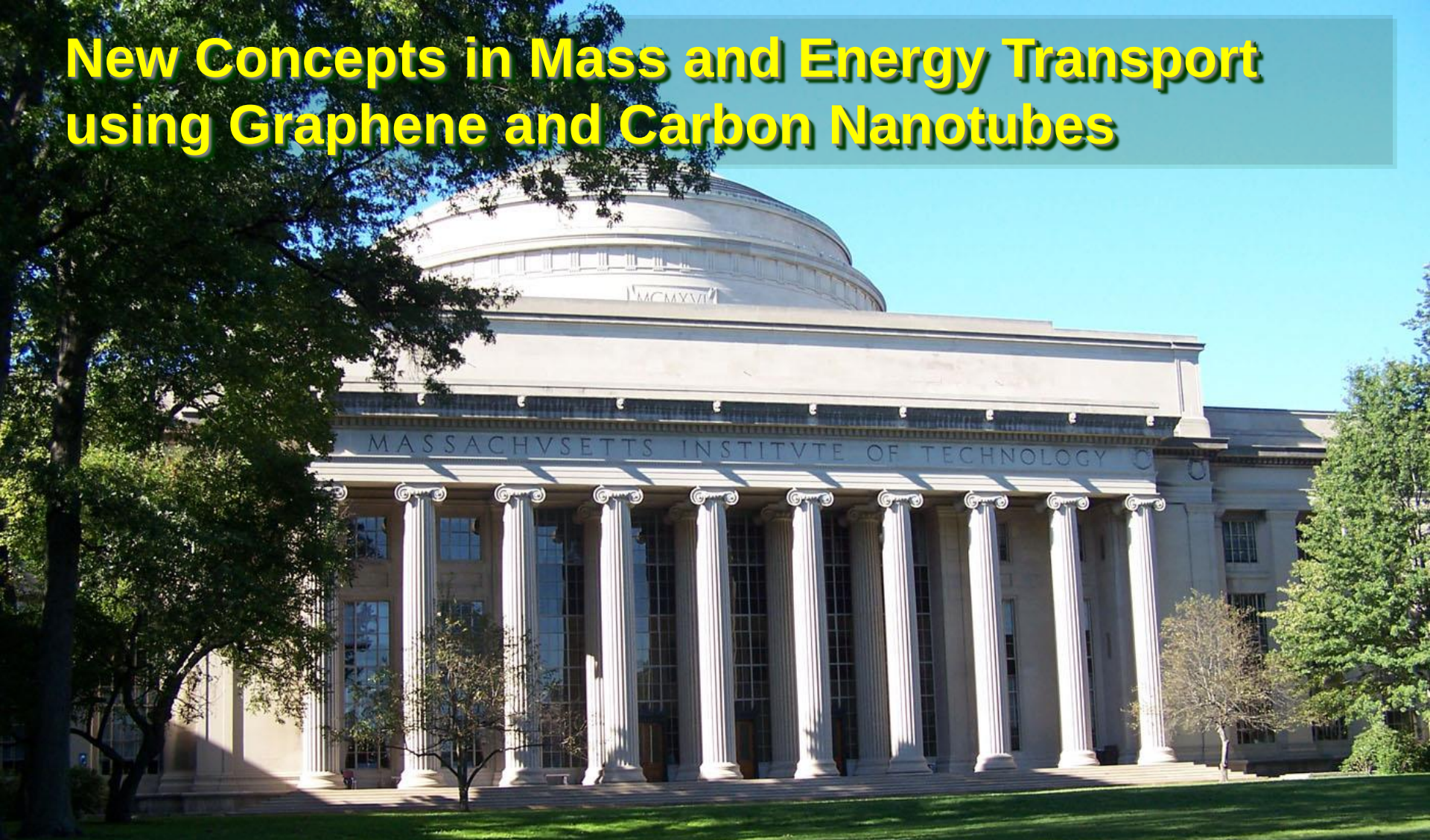

Michael S. Strano

Department of Chemical Engineering

Massachusetts Institute of Technology

W. Choi, C. Y. Lee, J. Abrahamson, N. Nair, C. Song, J. H. Han, G. Paulus, A. Boghossian

Carbon Nanotubes and Graphene

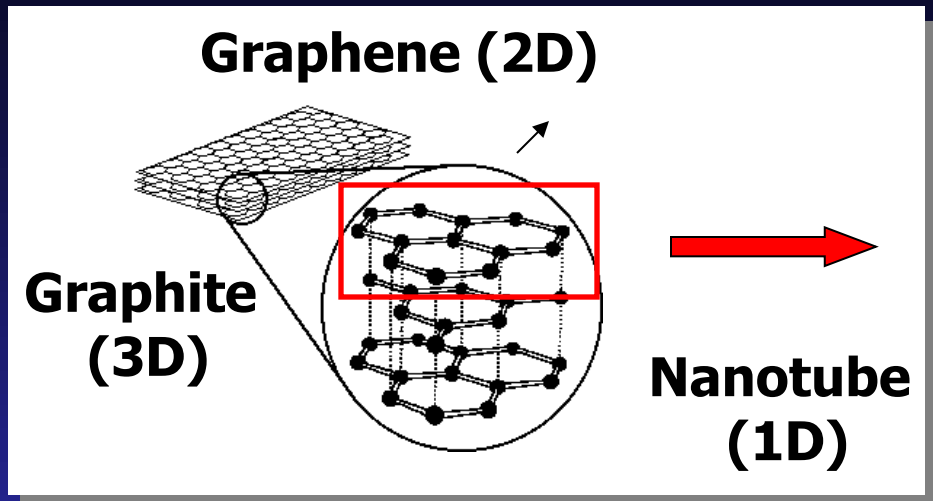

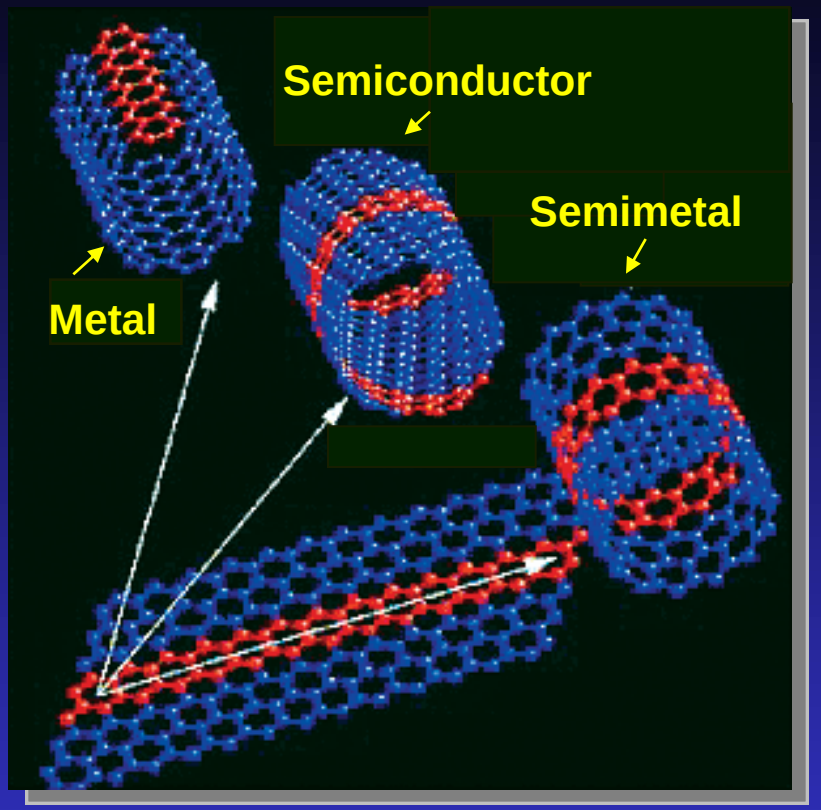

Electrons restricted to single dimension
Diameter ~1 nm

Synthesis (now > 1000 tons/year)
Stratis V. Sotirchos: electric arc synthesis
Over metal (Fe, Co, Mo) nanoparticle

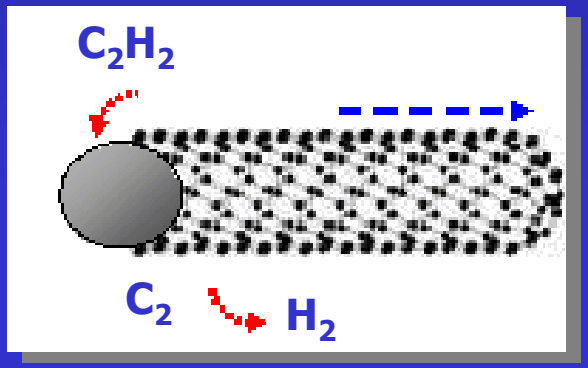

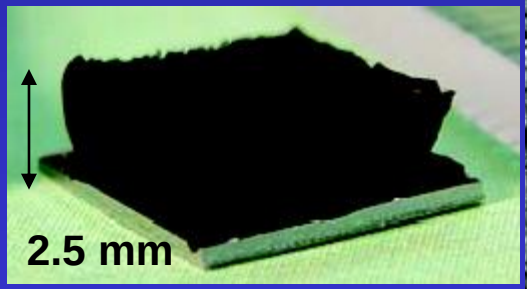

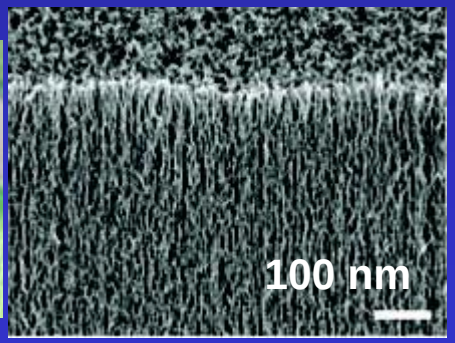

Length can range from 10 nm to 1 cm

Hata, K., Science 306, (2004), 1362

Diversity of Electronic Structure

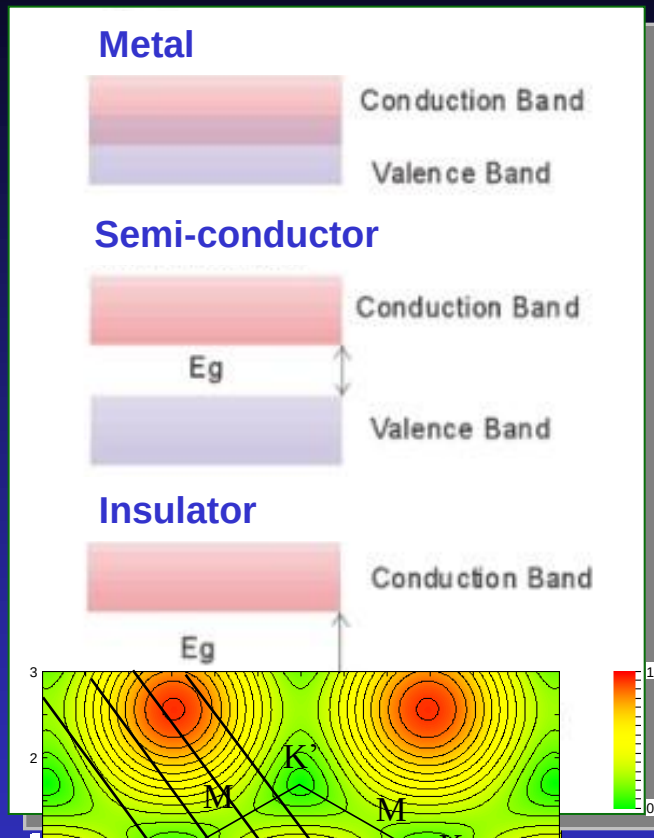

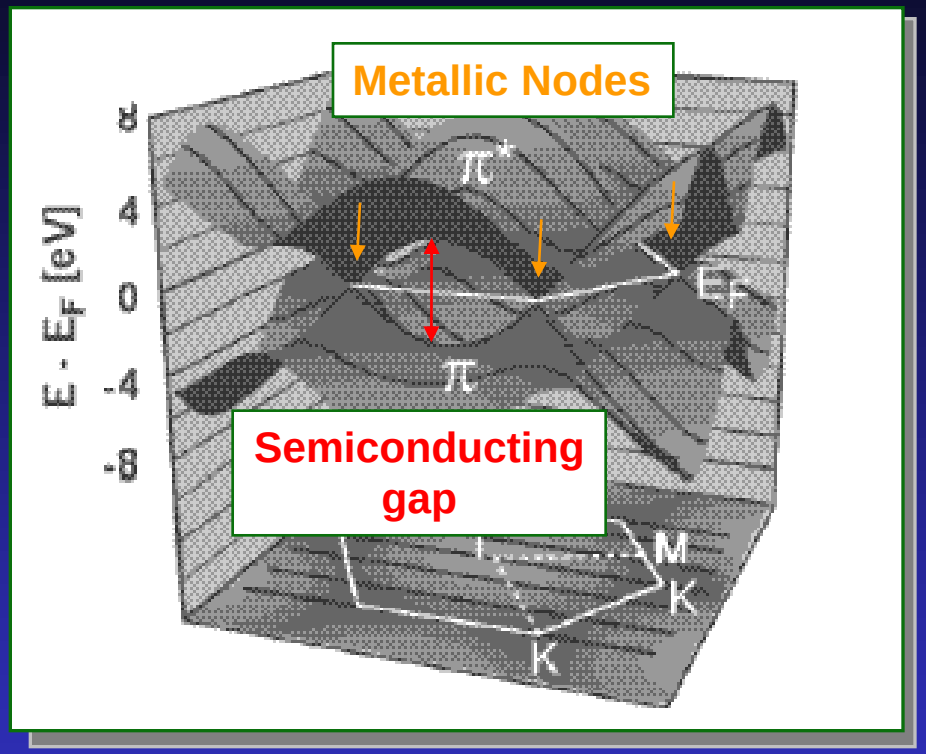

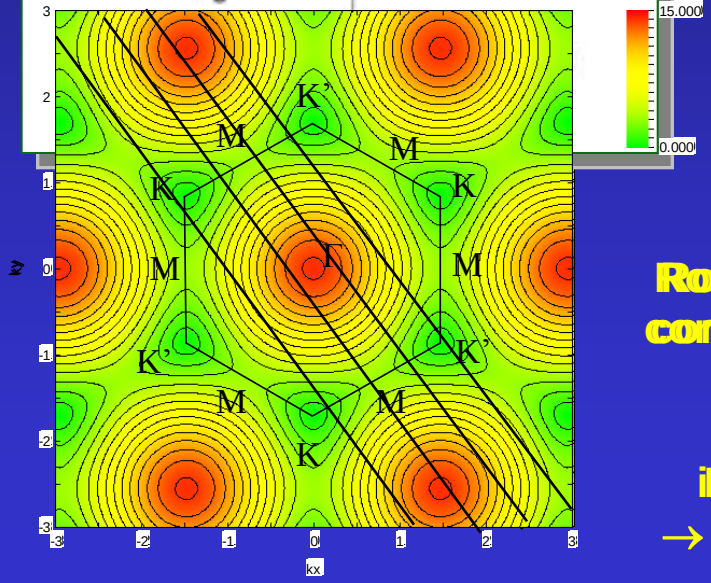

Rolling into cylinder constrains electrons to 1-D

Interacts K point
→ semiconducting

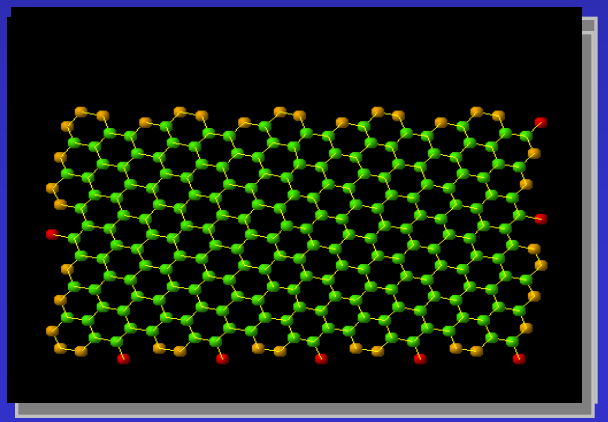

The Chirality Vector (n,m)

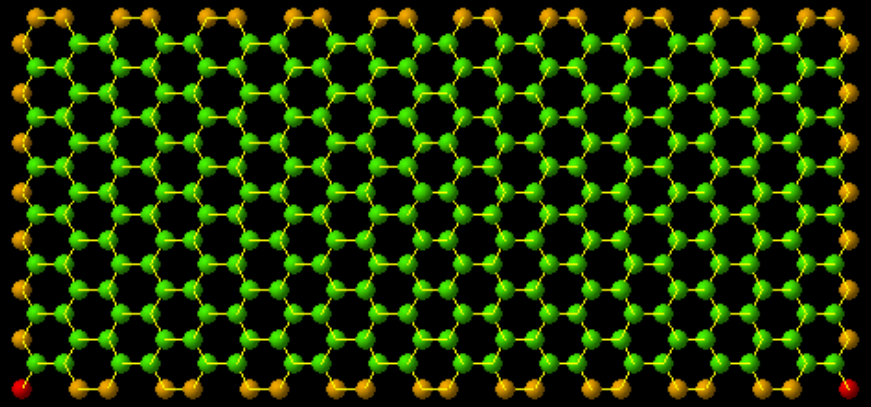

(10,10)

(n,m) where n = m

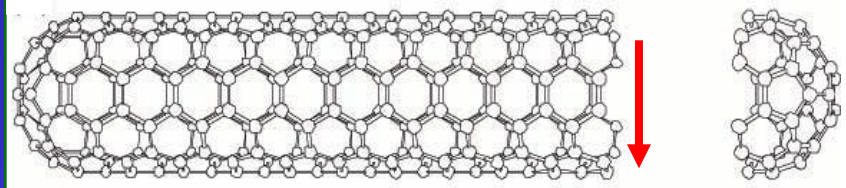

"armchair" nanotube, 1-D metal
if (n – m)/3 = integer then metallic

Energy (eV)

(10,5)

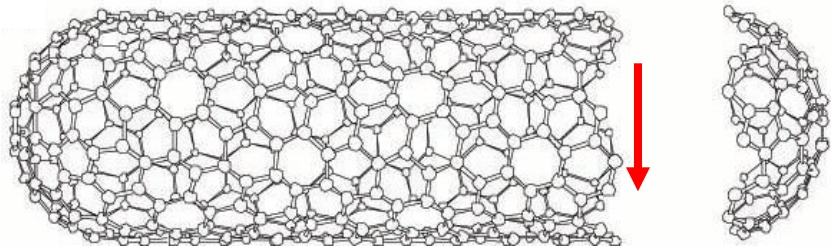

chiral nanotube, 1-D metal or
semiconductor if (n – m)/3 ≠ integer

Energy (eV)

Construction of Nanotubes from a Graphene Sheet

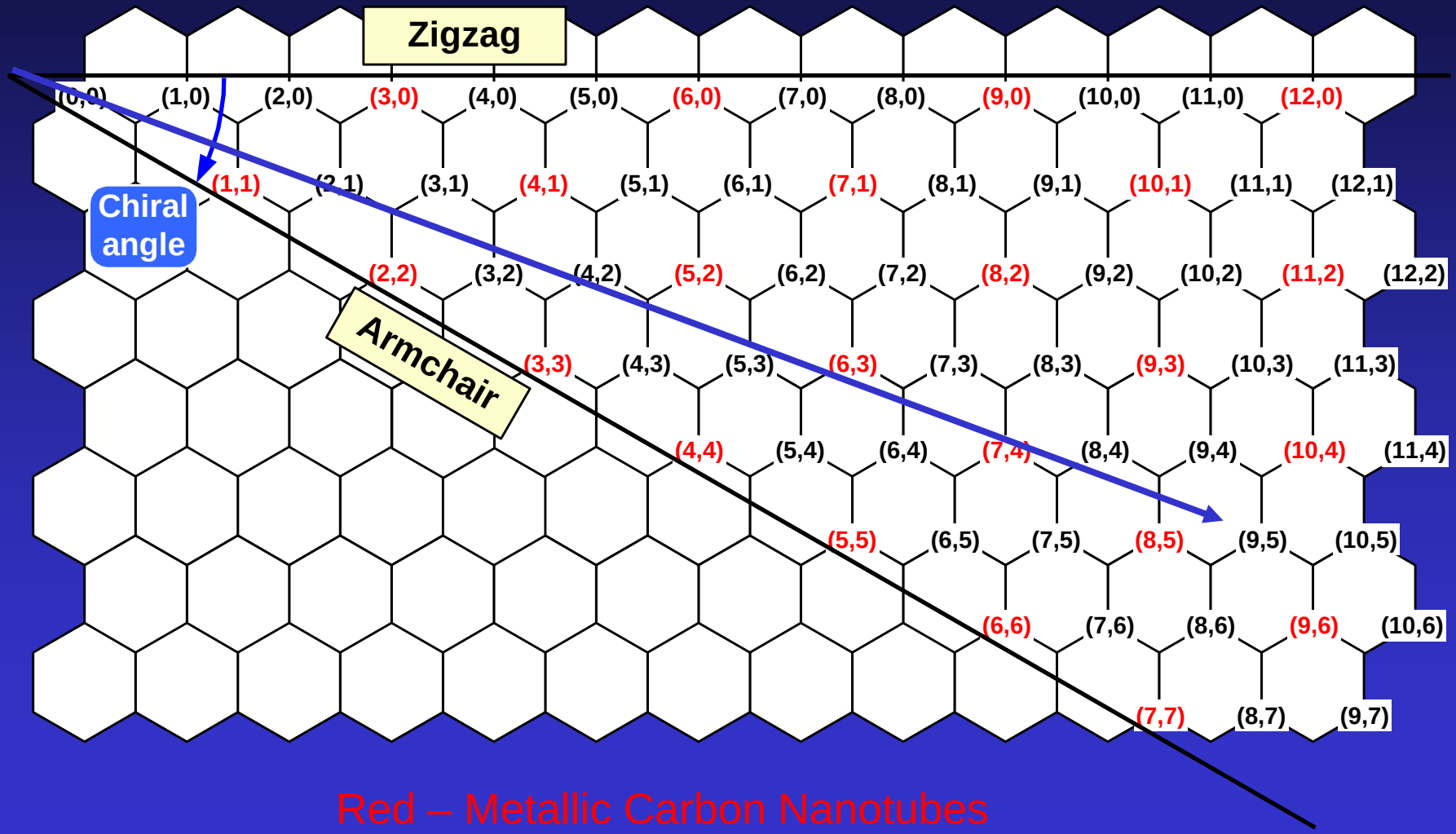

Red – Metallic Carbon Nanotubes

Black – Semi-conducting Carbon Nanotubes

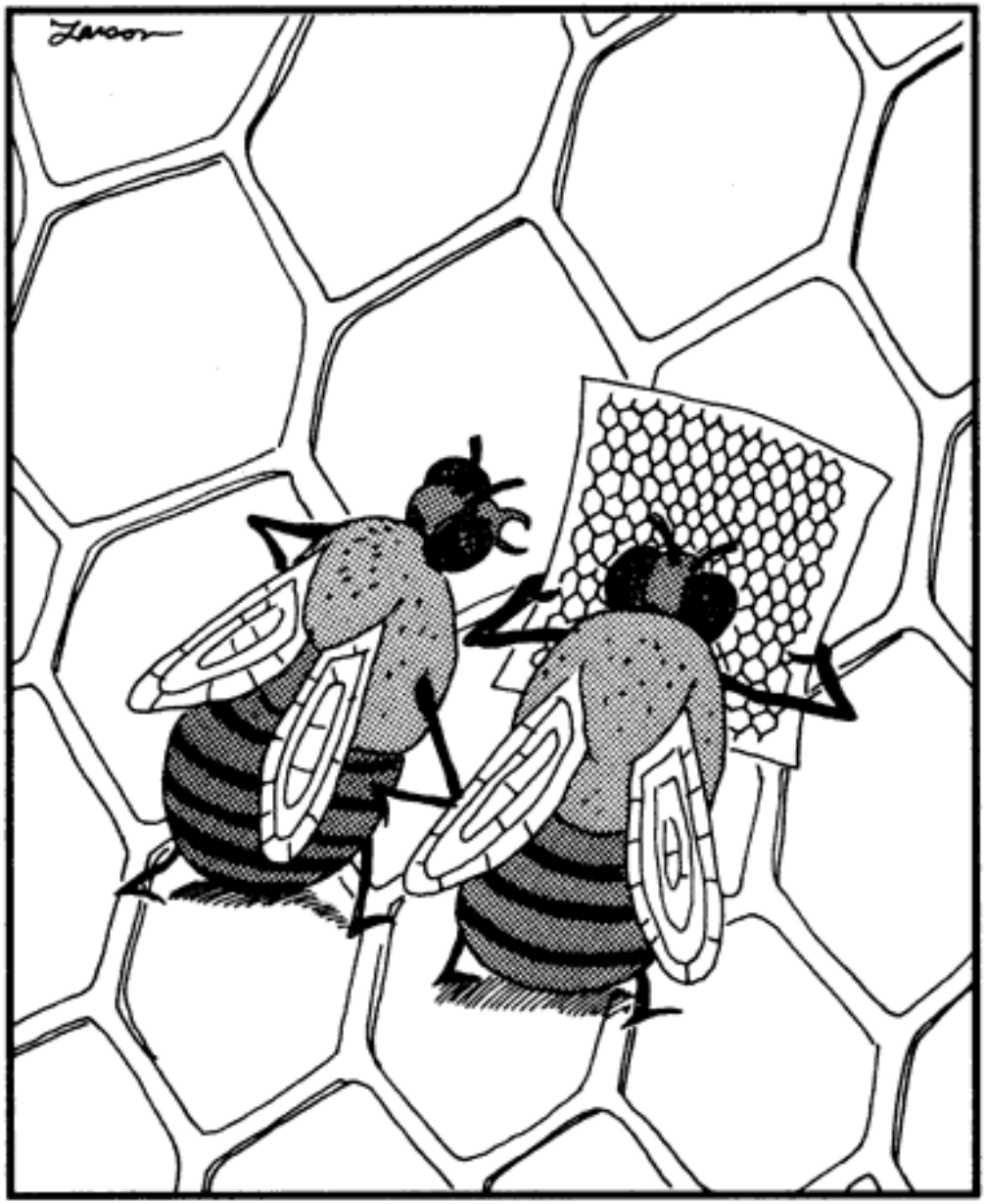

"Face it, Fred—you're lost!"

Applications of Graphene and Carbon Nanotubes

Ideal Molecular Wires and Films

High current density 10^9 **A/cm^2 or 30 μA per nanotube**
High electron mobility 20,000 cm^2/V/s

V. Perebeinos, J. Tersoff, and Ph. Avouris,
Phys. Rev. Lett. **94**, 086802 (2005).

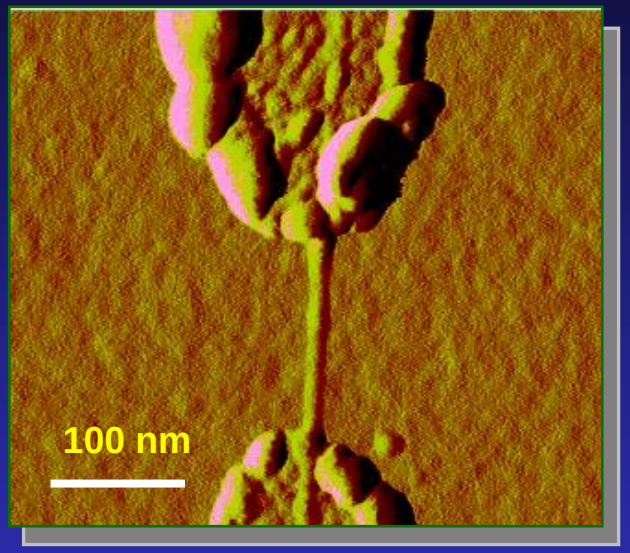

Unique Field Effect Transistors

Graphene bilayers – tunable bands

Shih, C. J. and Strano, M.S. Nanoletters (2013) in press.
Shih, C. J. and Strano, M. S. Langmuir, 28, 22 (2012) 8579

Near Infrared Absorption/Emission

Tissue implantable SWNT glucose sensors

Barone, P. and Strano, M. S. Nature Materials (2005)
Yoon, H. and Strano, M. S. Angewandte Chemie 50, 8 (2011) 1828

Structural Applications

High elastic modulus 1 TPa
Highest strength to weight ratio

Salvetat, J. P, et. al. *Physical Review Letters* **1999**,*82*, 944-947.

Applications of Graphene and Carbon Nanotubes

Ideal Molecular Wires and Films

High current density 10^9 **A/cm²** **or 30 μA per nanotube**
High electron mobility 20,000 cm²/V/s

V. Perebeinos, J. Tersoff, and Ph. Avouris,
Phys. Rev. Lett. **94**, 086802 (2005).

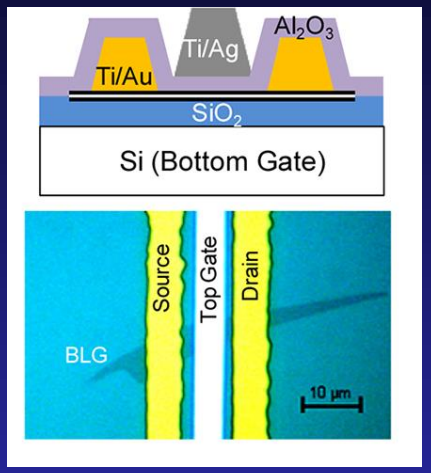

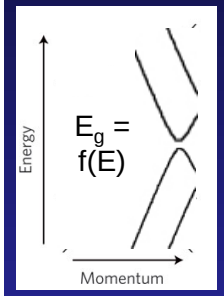

Unique Field Effect Transistors

Graphene bilayers – tunable bands

Shih, C. J. and Strano, M.S. Nanoletters (2013) in press.
Shih, C. J. and Strano, M. S. Langmuir, 28, 22 (2012) 8579

Near Infrared Absorption/Emission

Tissue implantable SWNT glucose sensors

Barone, P. and Strano, M. S. Nature Materials (2005)
Yoon, H. and Strano, M. S. Angewandte Chemie 50, 8 (2011) 1828

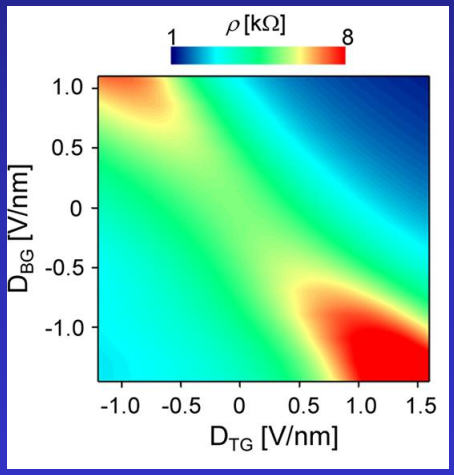

Structural Applications

High elastic modulus 1 TPa
Highest strength to weight ratio

Salvetat, J. P, et. al. *Physical Review Letters* **1999**,*82*, 944-947.

Applications of Graphene and Carbon Nanotubes

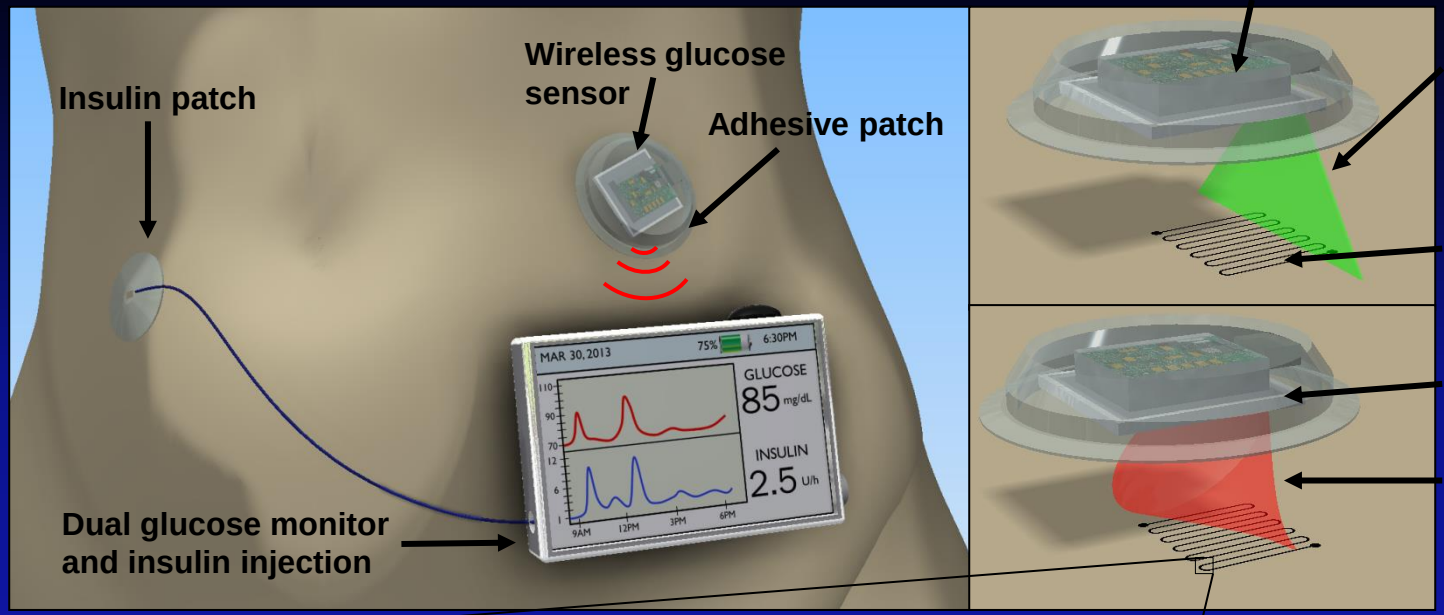

Alginate microparticles with carbon nanotubes

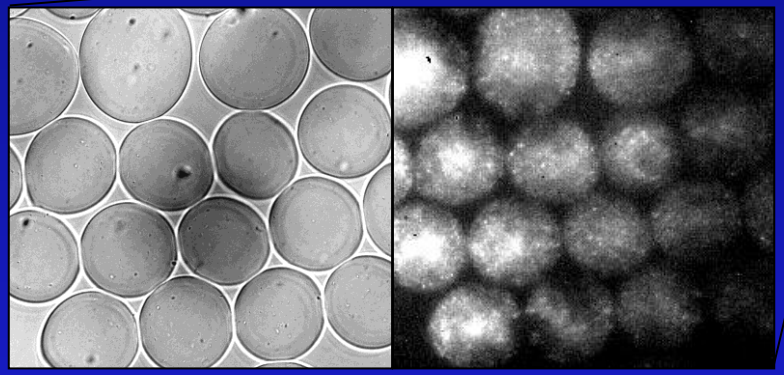

Optical

nIR Fluorescence

Applications of Graphene and Carbon Nanotubes

Ideal Molecular Wires and Films

High current density 10^9 **A/cm²** **or 30 μA per nanotube**
High electron mobility **20,000 cm²/V/s**

V. Perebeinos, J. Tersoff, and Ph. Avouris,
Phys. Rev. Lett. **94**, 086802 (2005).

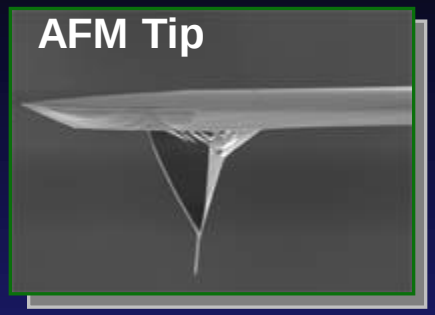

Unique Field Effect Transistors

Graphene bilayers – tunable bands

Shih, C. J. and Strano, M.S. Nanoletters (2013) in press.
Shih, C. J. and Strano, M. S. Langmuir, 28, 22 (2012) 8579

Near Infrared Absorption/Emission

Tissue implantable SWNT glucose sensors

Barone, P. and Strano, M. S. Nature Materials (2005)
Yoon, H. and Strano, M. S. Angewandte Chemie 50, 8 (2011) 1828

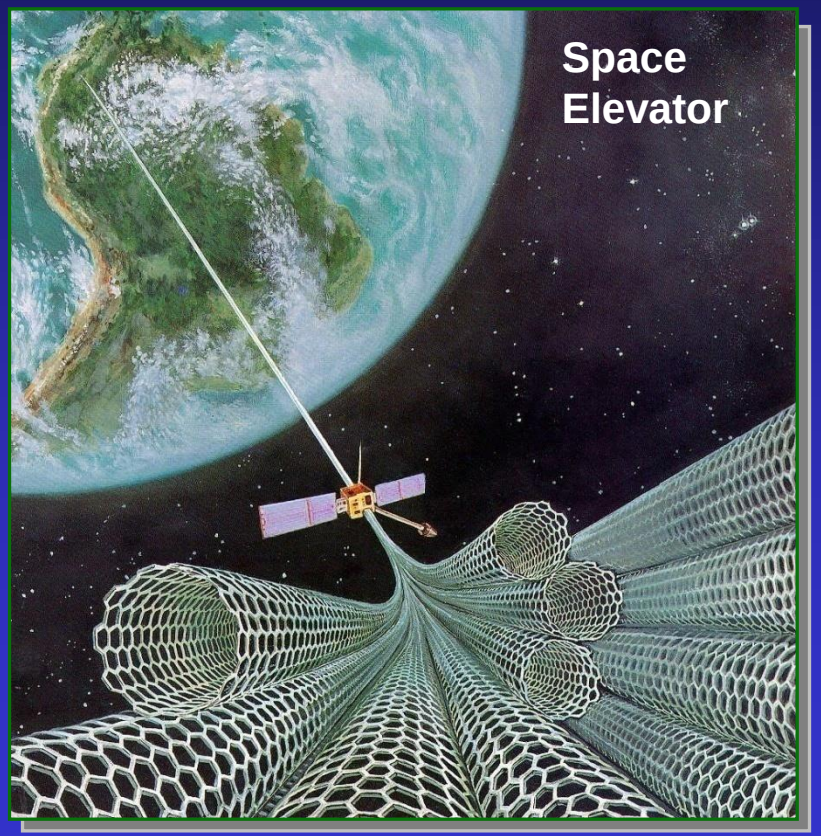

Structural Applications

High elastic modulus 1 TPa
Highest strength to weight ratio

Salvetat, J. P, et. al. *Physical Review Letters* **1999**,*82*, 944-947.

New Concepts in Mass and Energy Transport using Graphene and Carbon Nanotubes

- Coherence resonance in molecular transport through a single walled carbon nanotube nanopore

- Energy storage and generation using thermopower waves

- Near infrared fluorescent sensors with single molecule sensitivity for studying biological signaling fluxes: reactive oxygen and nitric oxide signaling in Epidermal Growth Factor Receptor (EGFR)

New Concepts in Mass and Energy Transport within Carbon Nanotubes

- Coherence resonance in molecular transport through a single walled carbon nanotube nanopore

- Energy storage and generation using thermopower waves

- Near infrared fluorescent sensors with single molecule sensitivity for studying biological signaling fluxes: reactive oxygen and nitric oxide signaling in Epidermal Growth Factor Receptor (EGFR)

Molecular Transport through a Single Nanotube

Substantial interest in understanding molecular transport within nanotubes

Most studies have been computational;
Many applications

- -Fuel cells membranes
- -Energy storage
- -DNA sequencing
- -Water desalination

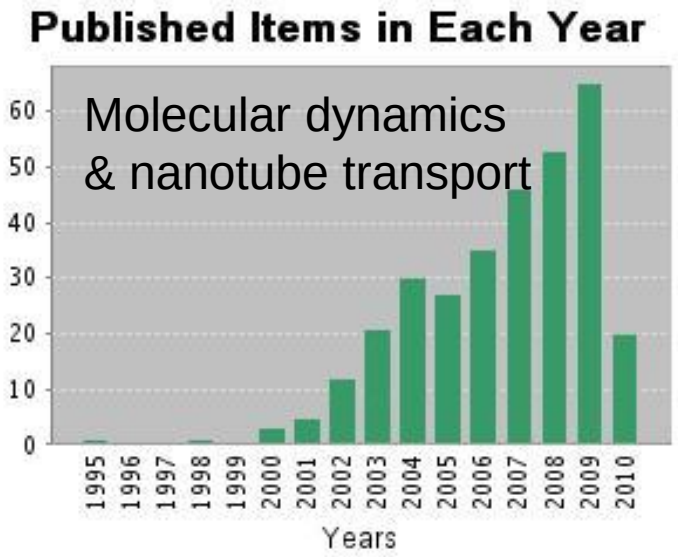

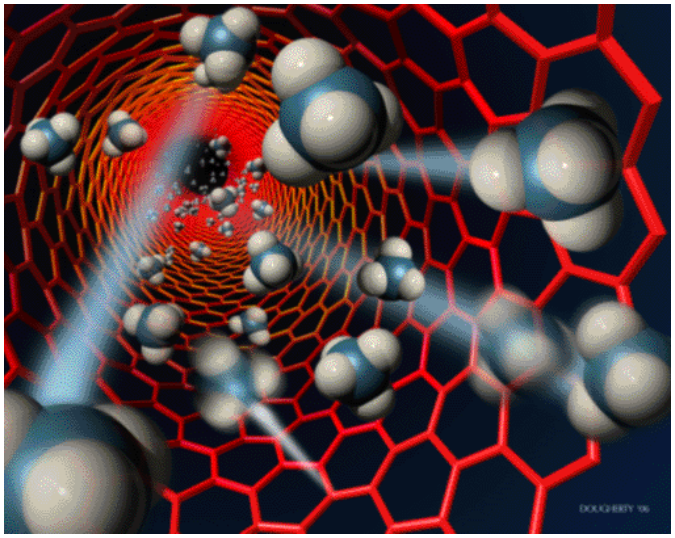

scitizen.com/.../slippery-nanopipes_a-5-131.html

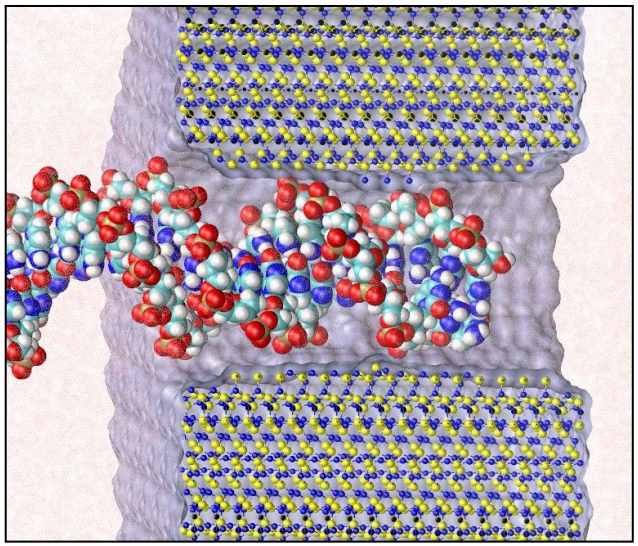

physics.illinois.edu/people/aksimentiev/

Creating and Characterizing SWNT Ion Channels

Lee, CY, Choi W, Han, JH, Strano MS: Science, 239, 1320 - 1324 (2010).
Choi, W., Shimizu, S., Strano, M.S. in preparation

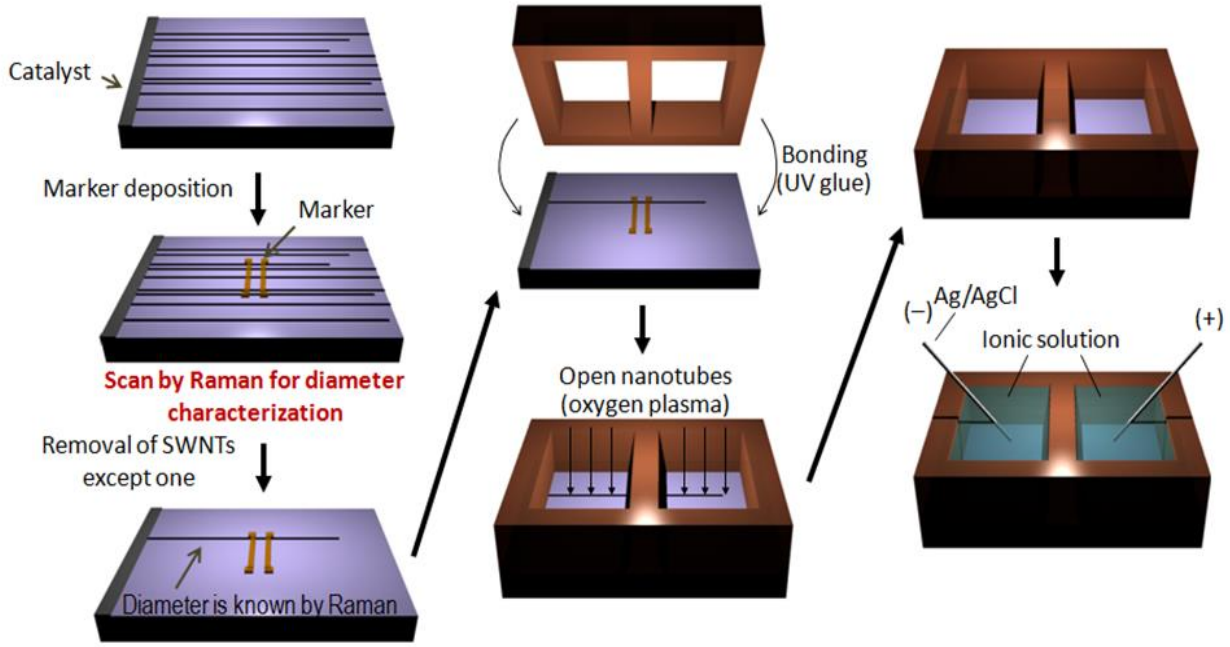

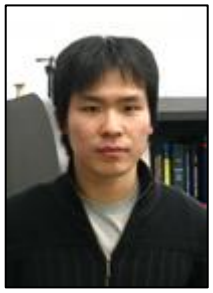

Won Joon Choi

Chang Young Lee

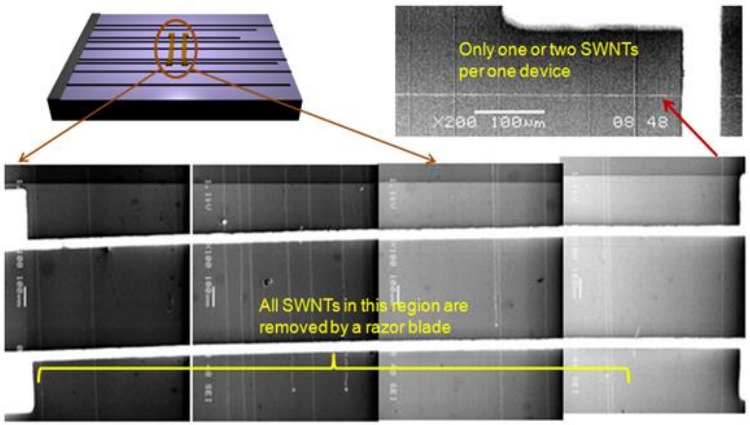

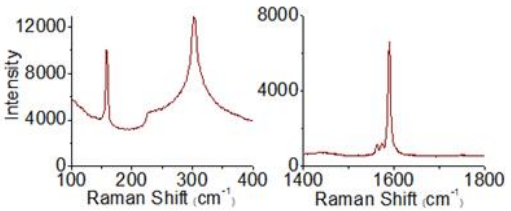

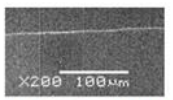

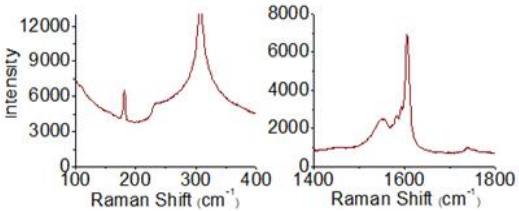

Ion Transport in the Nanotube Interior

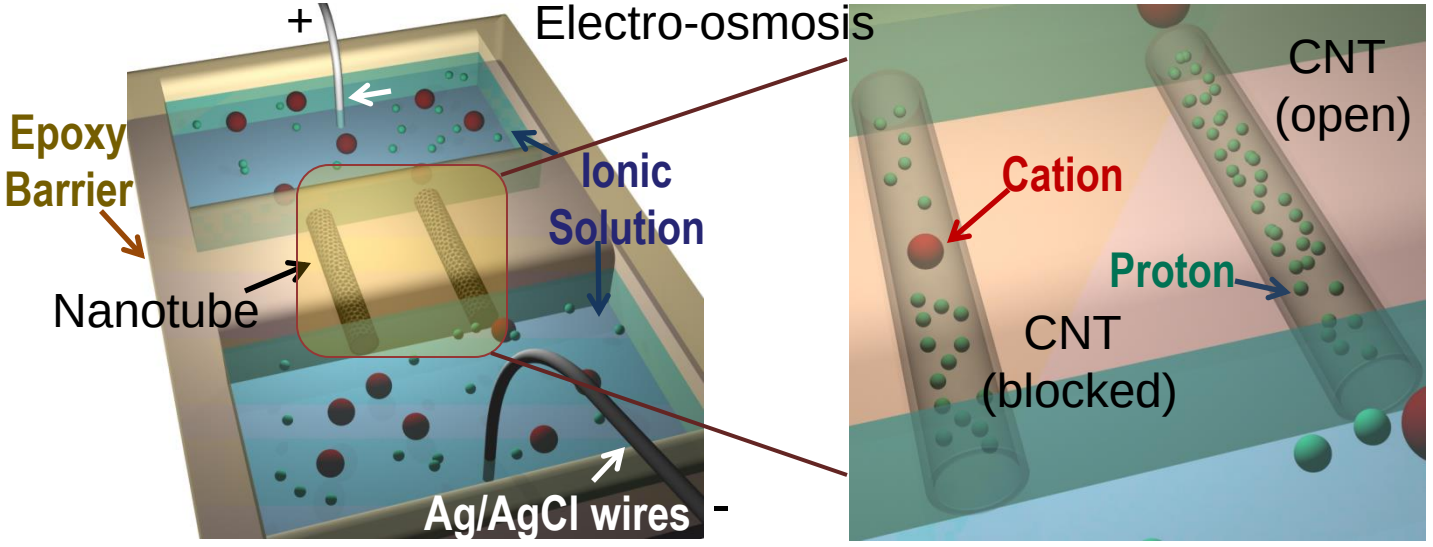

Pure Water (without electrolyte, 1000 mV)

KCl 3M (with electrolyte, 1000 mV)

Lee, CY, Science, 239, 1320 - 1324 (2010)

Stochastic Pore Transport: the Coulter Effect

Wallace H. Coulter
(1913-1998)

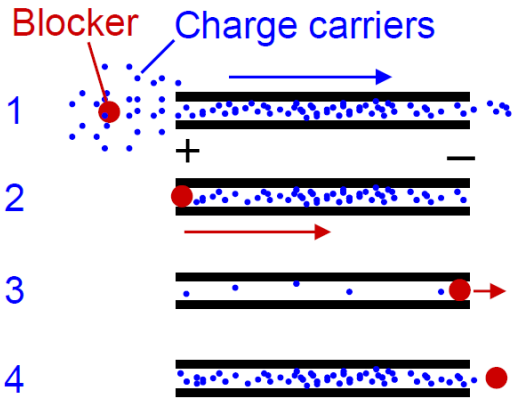

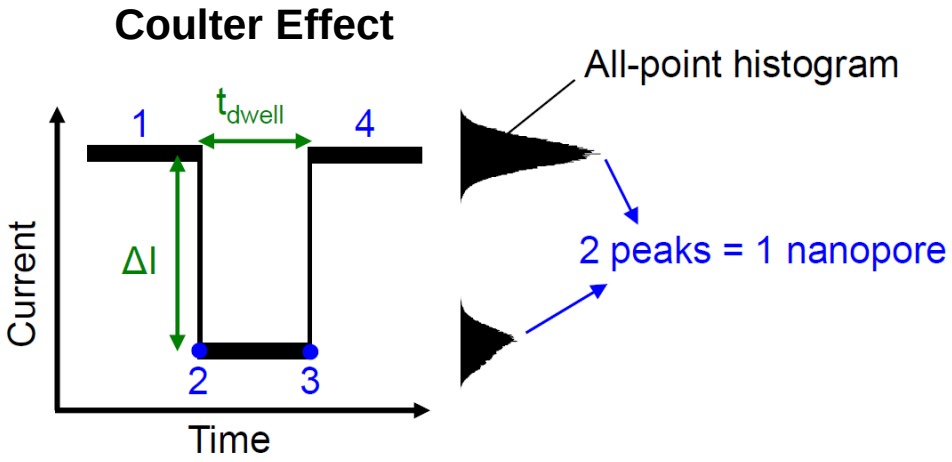

α-hemolysin pore

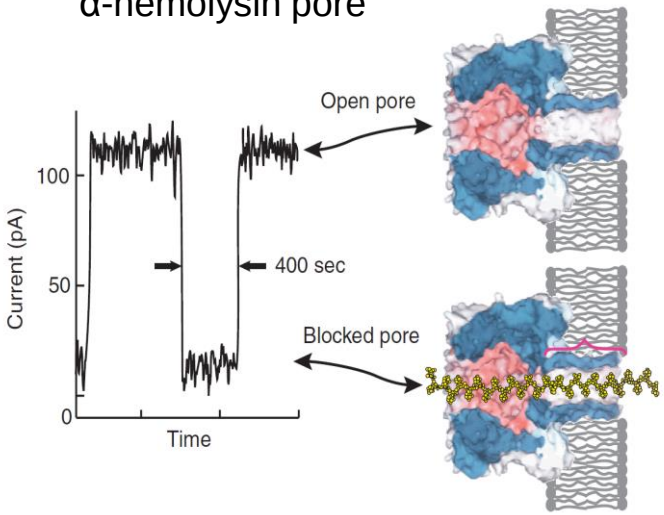

Analyte at different concentration

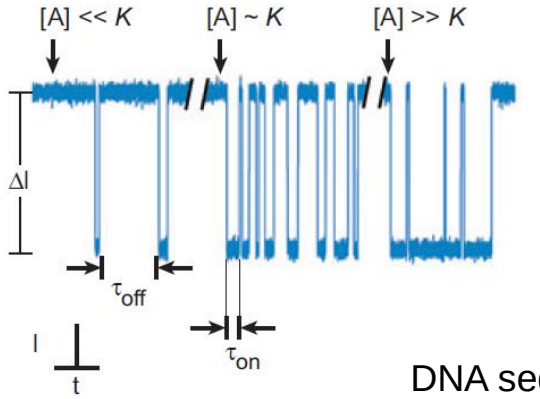

Ion channels from peptide nanotubes

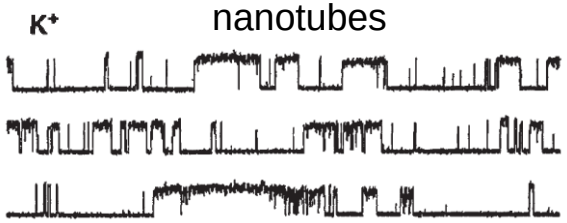

DNA sequencing by nanopore

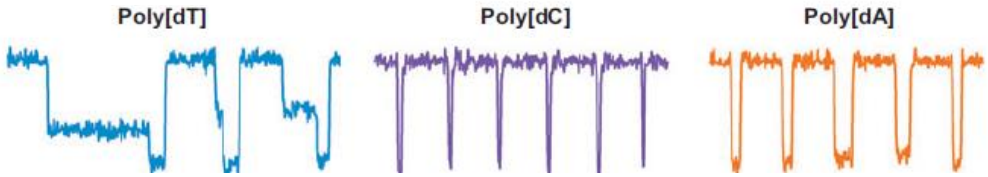

Branton et al. *Nature Biotech*, (2008) 26 (10) Kasianowicz et al. *Annu Rev Anal Chem*, (2008) 1 (737) Ghadiri et al. *Nature*, (1994) 369 (301)

Single Ion Transport through a Single Nanotube

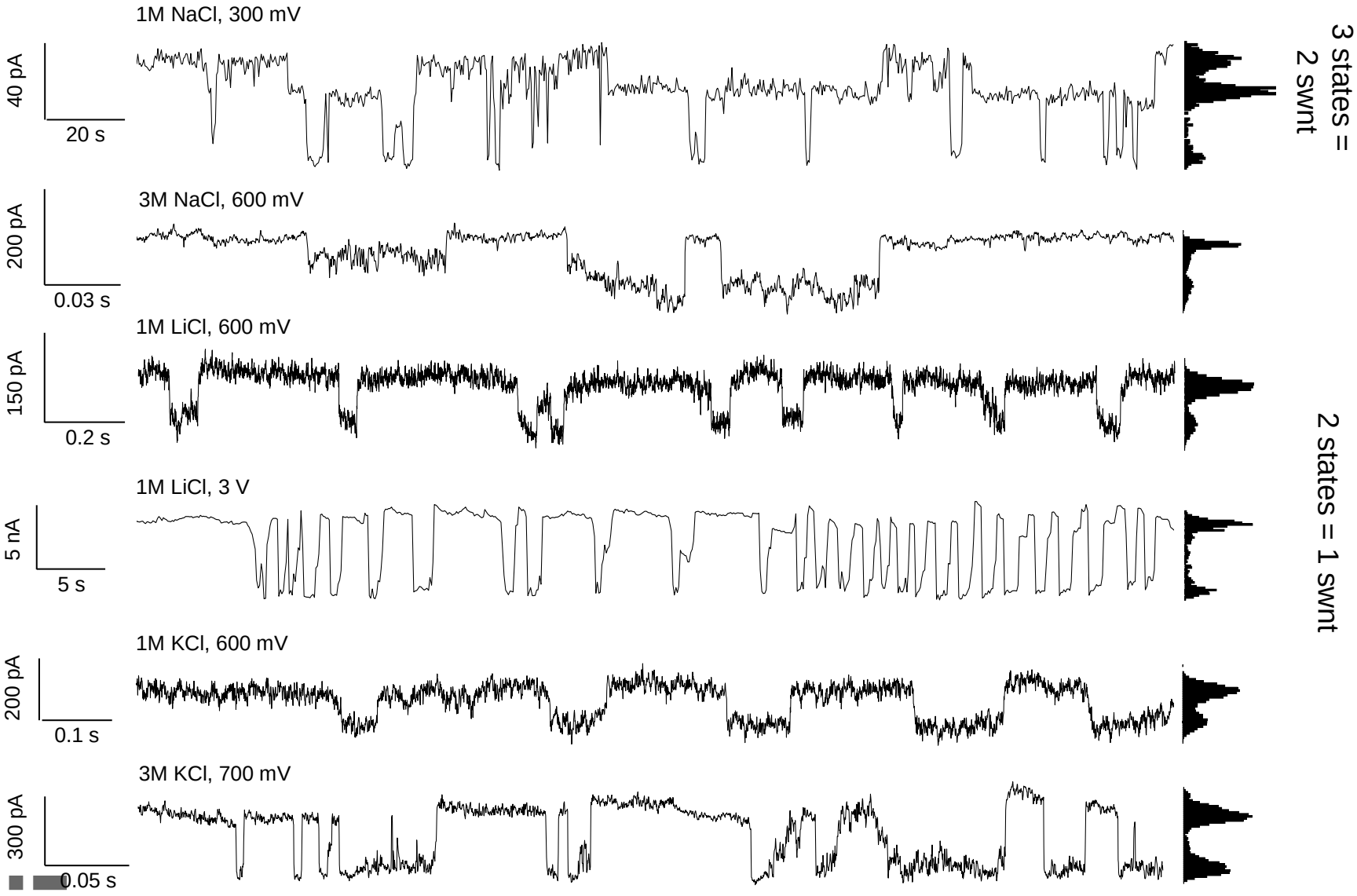

Lee, CY, Science, 239, 1320 - 1324 (2010)

Unblocked Current is Carried by Protons

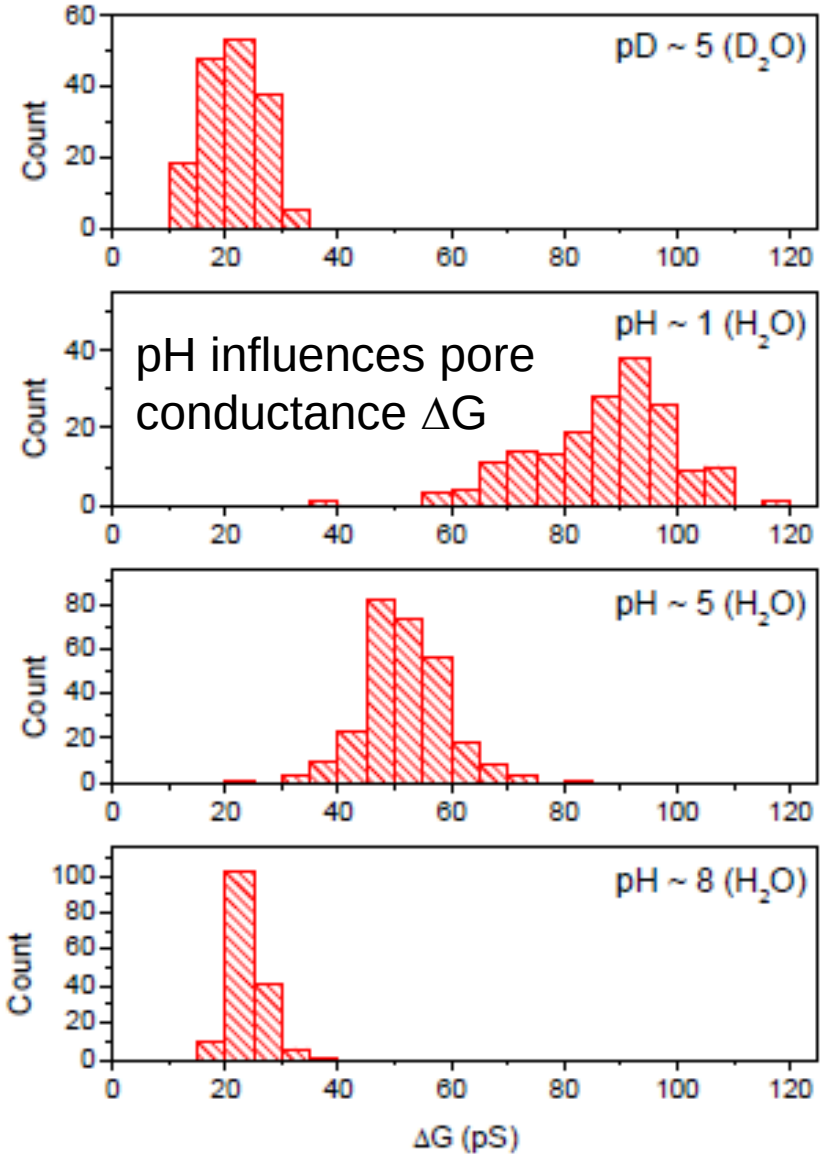

Measured $\Delta G_{H2O} / \Delta G_{D2O} = 2.5$

From acid/base titrations in bulk water (diffusion limited) = 1.6
(Pillings and Seakins, Reaction Kinetics, Oxford Science Press)

Cations block the nanotube

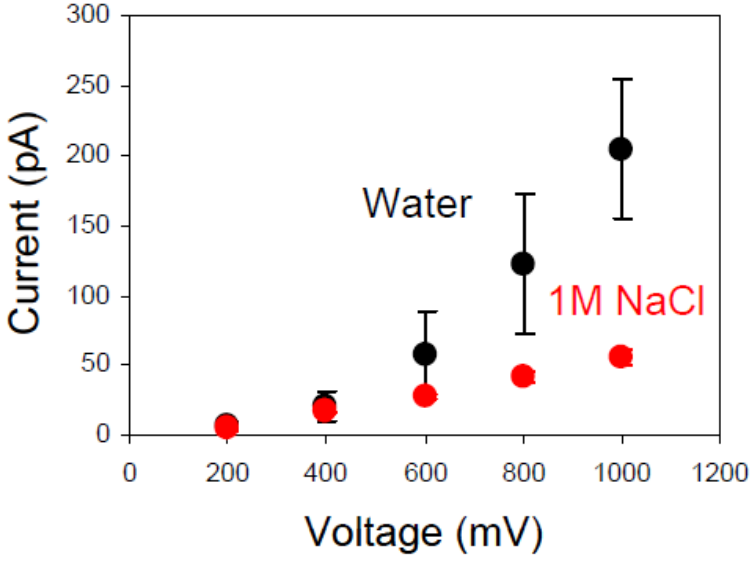

Lee, CY, Science, 239, 1320 - 1324 (2010)

Cations are the Blocking Species

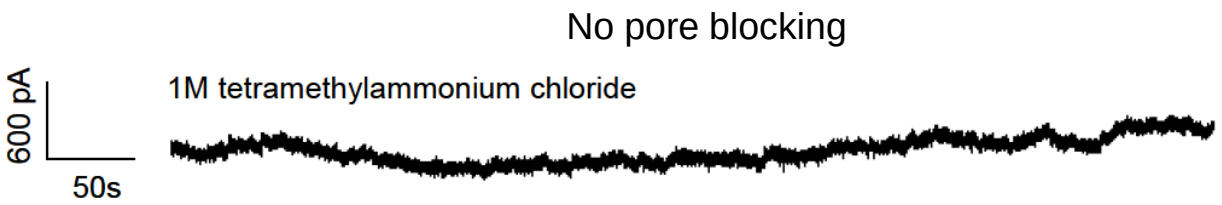

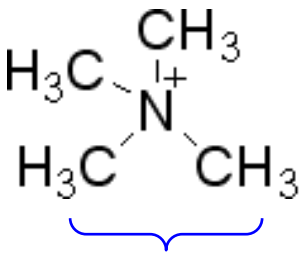

Anion cannot block Cl^-

No blocking events with tetramethylammonium chloride or hydrogen chloride

Large cation (d=0.7nm)

Note: only **cations** appear block the pore

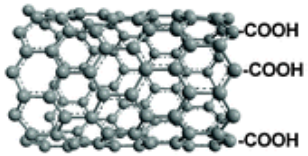

Hypothesis: plasma etch leaves residual carboxylic acid groups at pore ends (negative zeta potential)

Threshold potential observed for cation pore blocking

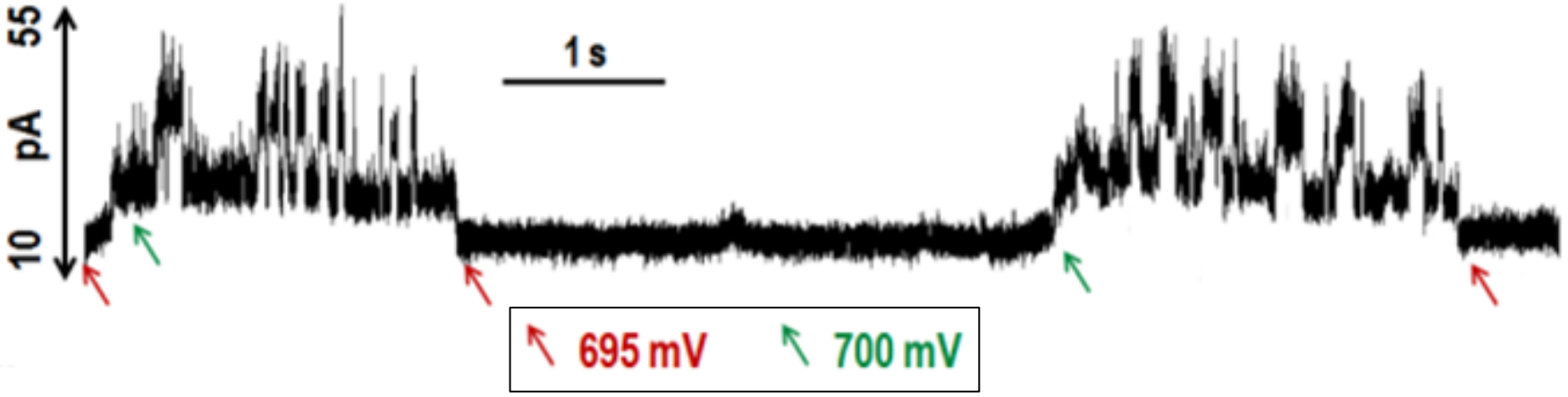

Choi W et al *J. Am. Chem. Soc*, (2011) 133 (203)

Theory: Molecular Transport in Nanotubes

Important theoretical/computational predictions (300+ since 2000)

Enhanced water permeation flux through carbon nanotubes

A. Alexiadis, S. Kassinos, *Chemical Reviews* **108**, 5014 (DEC, 2008).

Large proton fluxes through water filled carbon nanotubes

C. Dellago, M. M. Naor, G. Hummer, *Physical Review Letters* **90**, 105902 (Mar 14, 2003).

Ice-like water phase in carbon nanotube interior

K. Koga, G. T. Gao, H. Tanaka, X. C. Zeng, *Nature* **412**, 802 (Aug 23, 2001).

High ion rejection rates from nanotube interior

O. Beckstein, K. Tai, M. S. P. Sansom, *Journal of the American Chemical Society* **126**, 14694 (Nov 17, 2004).

Experimental: success with nanotube membranes

J. K. Holt *et al.*, *Science* **312**, 1034 (May 19, 2006).

F. Fornasiero *et al.*, *Proceedings of the National Academy of Sciences of the United States of America* **105**, 17250 (Nov 11, 2008).

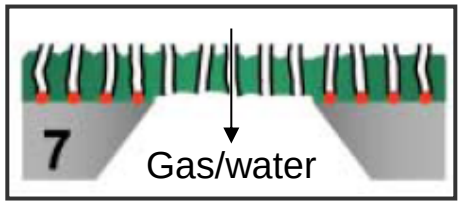

Holt et al. Science 312, 1034-1037 (2006)

Ion Translocation Follows Expected Nanopore Physics

- Current fluctuations for Ca^{2+} demonstrated trends expected for stochastic pore blocking

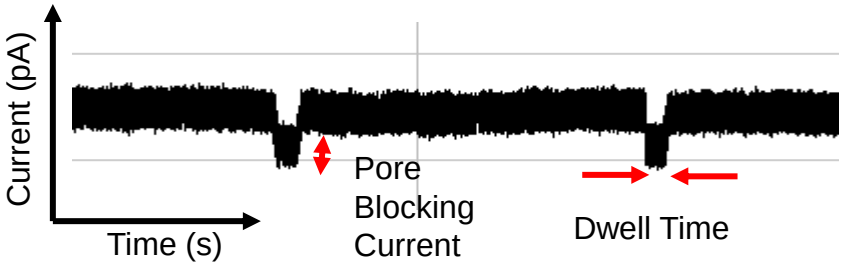

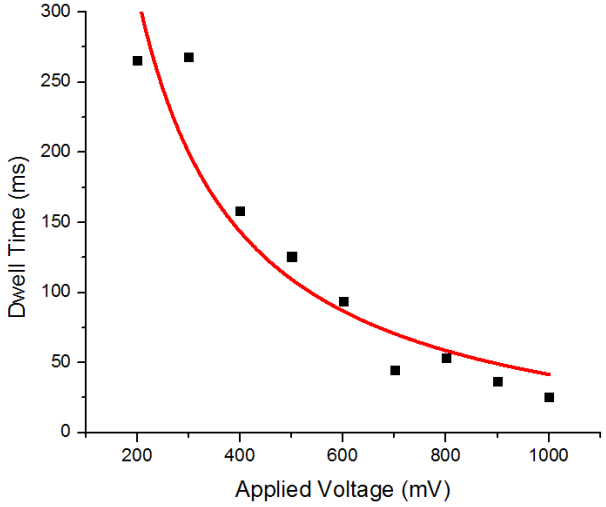

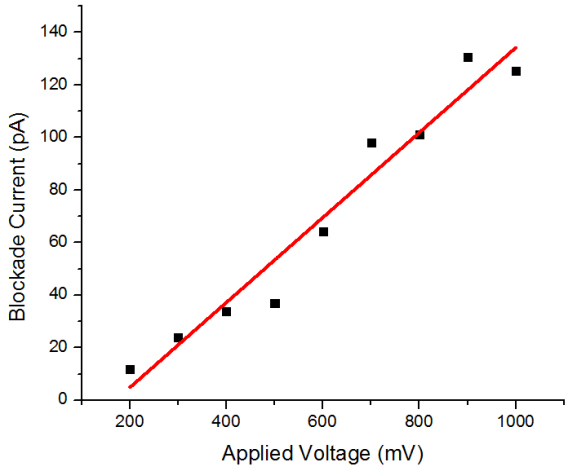

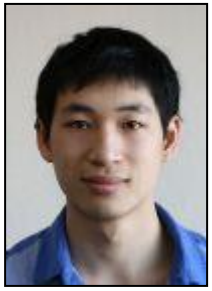

Steve Shimizu

Dwell time follows simple scaling of a single ion moving through the nanotube:

$$\tau_{dwell,ion} = \frac{L^2}{\mu_{ion} \cdot (V - V_{threshold})} \propto \frac{1}{V}$$

$\tau_{dwell,ion}$ = Dwell Time of Ion (s)

L = length of barrier (nanotube) (m)

V = applied voltage (V)

μ_{ion} = ion mobility inside nanotube (m^2/V-s)

Pore blocking current scales linearly with applied voltage:

$$I_{blocking} = \frac{q}{\tau_{H^+}} = \frac{q \cdot \mu_{H^+} \cdot (V - V_{threshold})}{L^2} \propto V$$

$I_{blocking}$ = pore blocking current (pA)

q = charge on H^+ (C)

τ_{H^+} = average residence time of H^+ inside the nanotube (s)

μ_{H^+} = H^+ mobility inside nanotube (m^2/V-s)

$V_{threshold}$ = threshold voltage at which pore blocking observed (V)

Proton Conductivity of a Nanotube

Proton conductivity is unusually large x 10^4 compared with sputtered Si ion channels

Blocking current ~ 100 pA = 6.25x10^8 protons/s gramicidin (biological) proton channel = 2.2 x 10^9 protons/s (at low pH)

Highly efficient conduction mechanism – "hop-and-turn" Grotthuss mechanism along the water chain

N. Agmon, *Chemical Physics Letters* **244**, 456 (Oct 13, 1995).

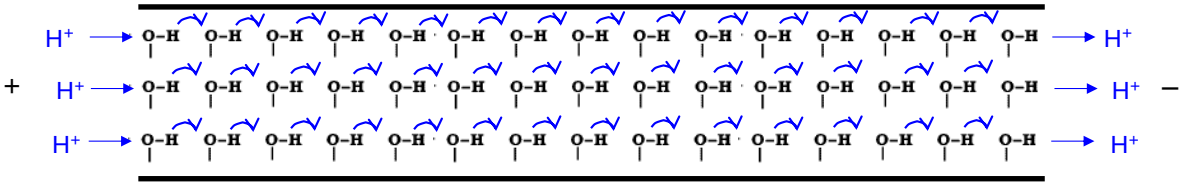

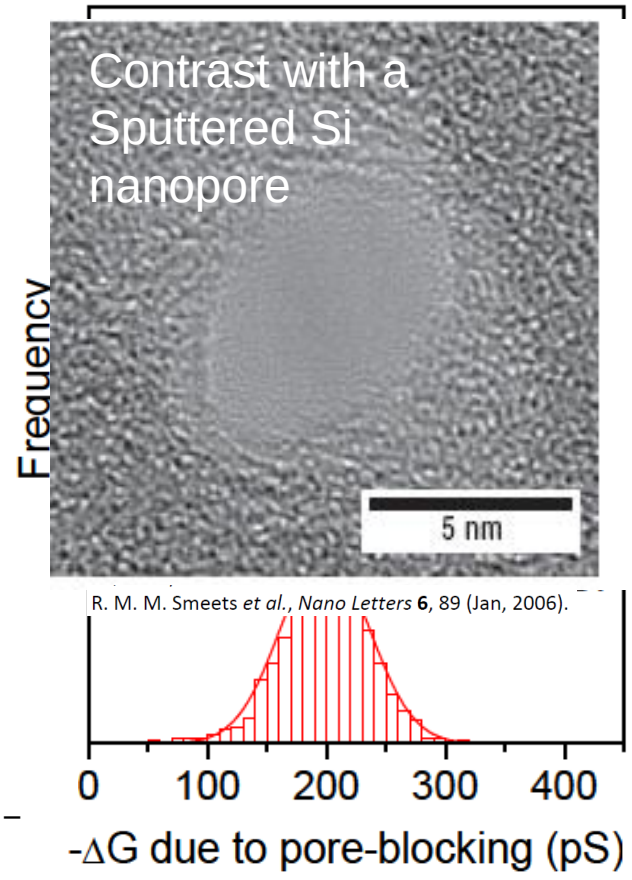

Divide by linear water density in tube 33/nm yields hopping velocity of 0.02 m/s and mobility of 2x10^{-5} $m^2/V/s$ at E = 10^3 V/m or x 100 bulk water.

Lee, CY, Science, 239, 1320 - 1324 (2010)

Blockade Current and Dwell Time Dependence on Ion Type

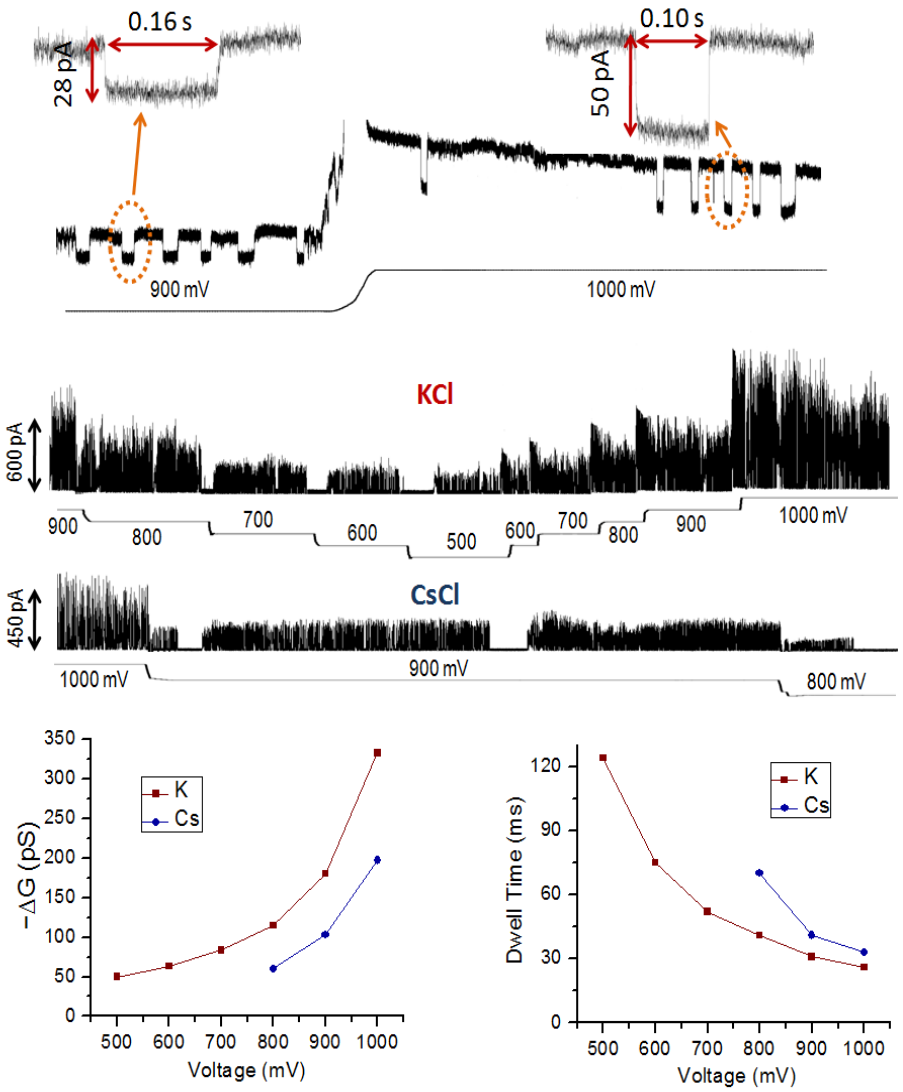

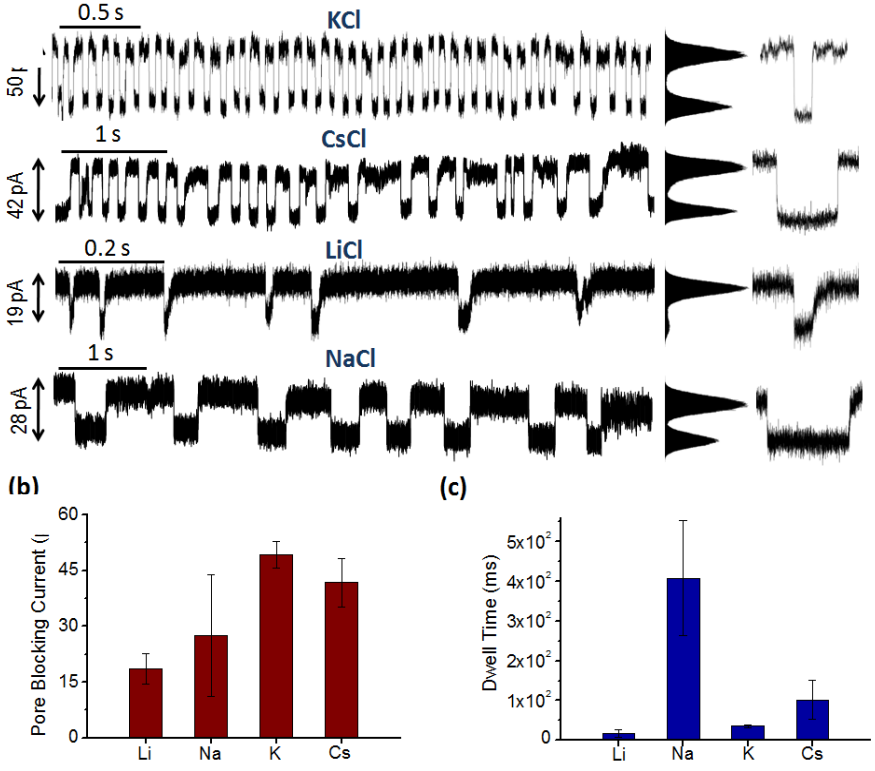

Summary

Dwell time: $Na^+ > Cs^+ > K^+ > Li^+$

Blockade Current: $K^+ > Cs^+ > Na^+ > Li^+$

Blockade Current vs Diameter Shows Maximum

THE JOURNAL OF CHEMICAL PHYSICS **124**, 174714 (2006)

Hydrogen bond dynamics and microscopic structure of confined water inside carbon nanotubes

Itsuo Hanasaki[a] and Akihiro Nakatani[b]
Department of Adaptive Machine Systems, Graduate School of Engineering, Osaka University, 2-1 Yamadaoka, Suita, Osaka 565-0871, Japan

(Received 28 September 2005; accepted 16 March 2006; published online 5 May 2006)

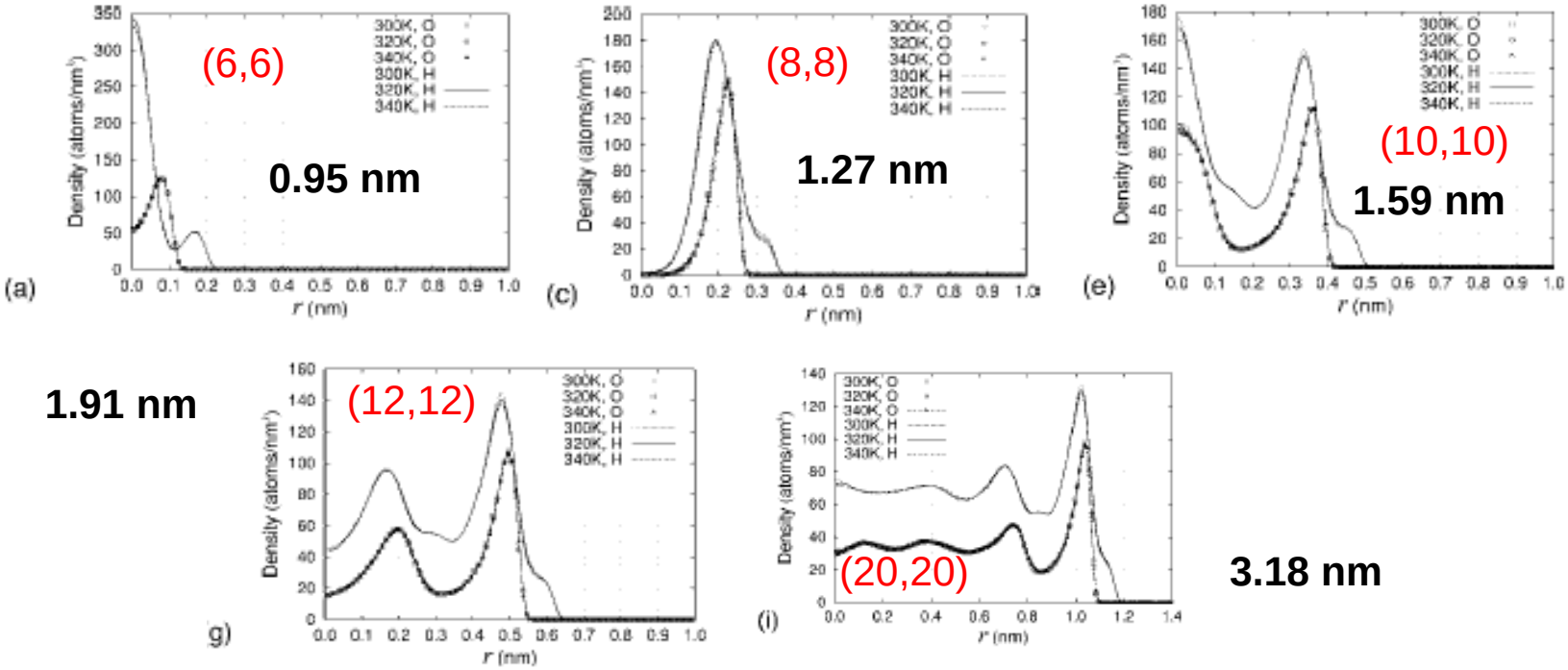

Water density increases strongly with decreasing diameter

Coordinated Molecular Transport

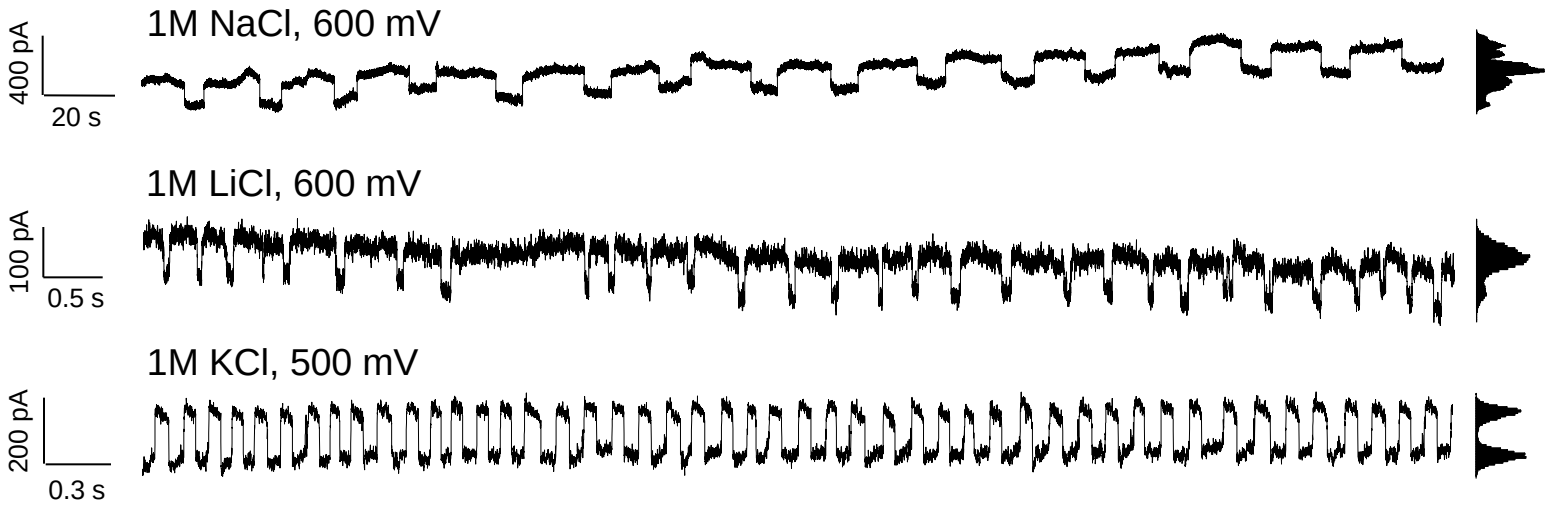

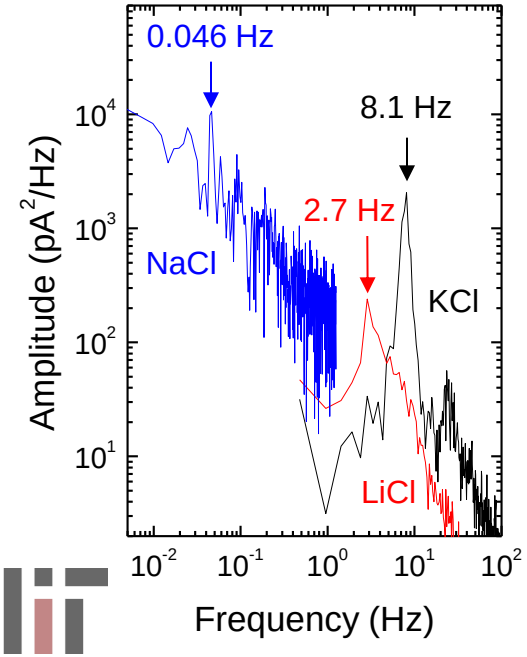

Coherent oscillation

- Under some conditions, electro-osmotic current can become synchronized for a duration of up to several minutes.
- Never previously reported for any synthetic nanopore system
- Clearly arises from a single nanotube
- FFT of output current displays unique coherence of transport 46 mHz to 8.1 Hz, ion dependent

Lee, CY, Science, 239, 1320 - 1324 (2010)

Resonant, Synchronized Transport

1 M KCl,
500 mV

Lee, CY, Science, 239, 1320 - 1324 (2010)

Stochastic Simulation Explains the Oscillation

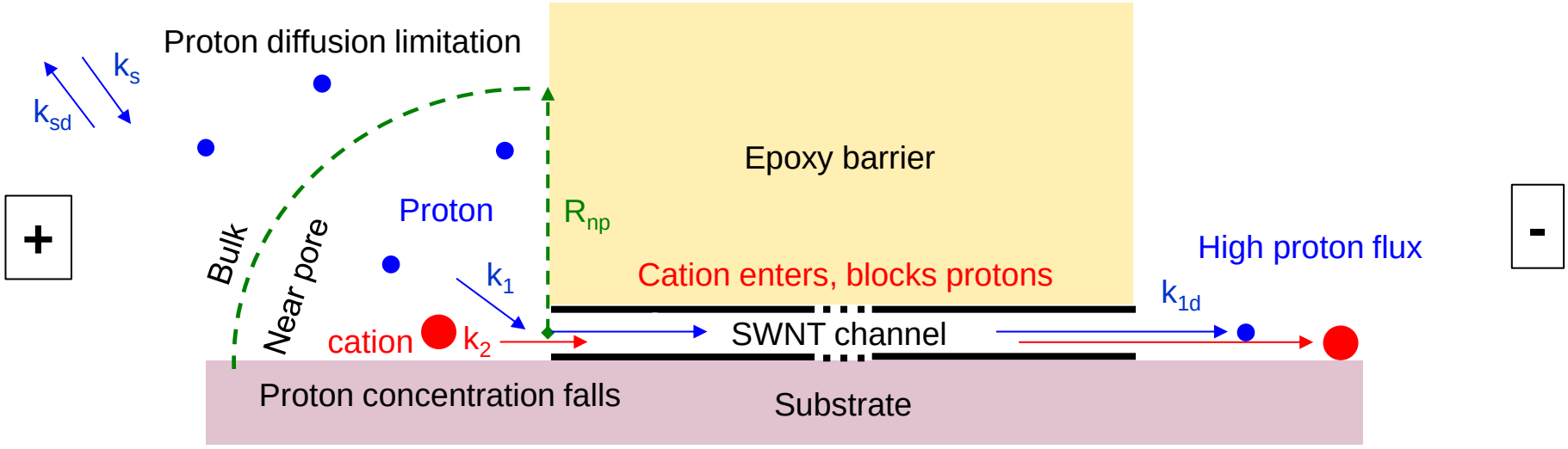

Mechanism can be simulated via 6 stochastic differential equations

1) $H_{np} + T \xrightarrow{k_1} H_{tube}$ (proton in)

2) $I_{np} + T \xrightarrow{k_2} I_{tube}$ (ion in)

3) $H_{tube} \xrightarrow{k_{1d}}$ (proton out)

4) $I_{tube} \xrightarrow{k_{2d}}$ (ion out)

5) $H_{bulk} \xrightarrow{k_s} H_{np}$

6) $H_{np} \xrightarrow{k_{sd}} H_{bulk}$

(proton exchange)

T = open nanopore state

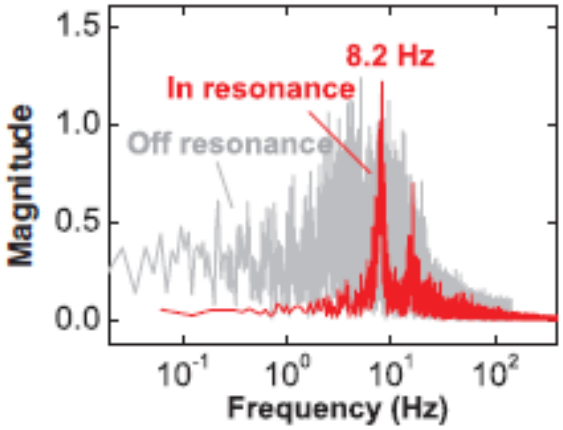

Lee, CY, Science, 239, 1320 - 1324 (2010)

Summary and Future Work – Ion Transport

- Carbon nanotube: new experimental conduit to manipulate single molecules in a nano-confined channel; test computational predictions

- Coherence resonance – dramatically increases the throughput of a nanopore sensor (x 100)

- Confined reactions and reactors, molecular synthesis and catalysis one molecule at a time

- Trace ion detection and ion separation in aqueous phases

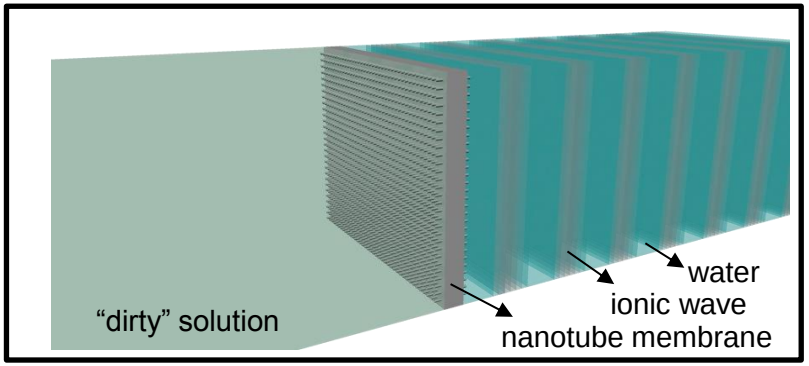

New Concepts in Mass and Energy Transport within Carbon Nanotubes

- Coherence resonance in molecular transport through a single walled carbon nanotube nanopore

- Energy storage and generation using thermopower waves

- Near infrared fluorescent sensors [illegible] ecule sensitivity for studying biological sig[illegible] active oxygen and nitric oxide signaling in [illegible]th Factor Receptor (EGFR)

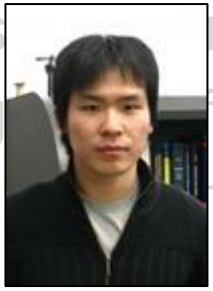

Won Joon Choi

Joel Abrahamson

Chemical Energy Densities are Much Larger than Electrochemical for Battery Applications

Electrochemical	Energy Density (MJ/L)
Li-ion	1.44
NiCd	0.72
NiMH	1.08
Chemical	
Ethanol	21.2
Glucose	24.0
Methane	22.2

Efficient, direct conversion of chemical to electrical energy is an unresolved problem.

Nanomaterials can demonstrate large anisotropic thermal conductivities

Quantum confinement suppresses phonon scattering mechanisms

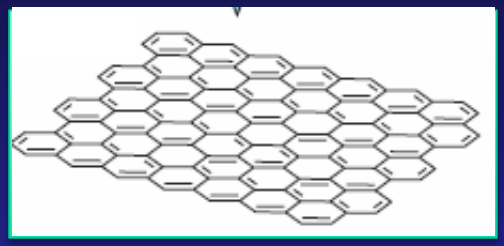

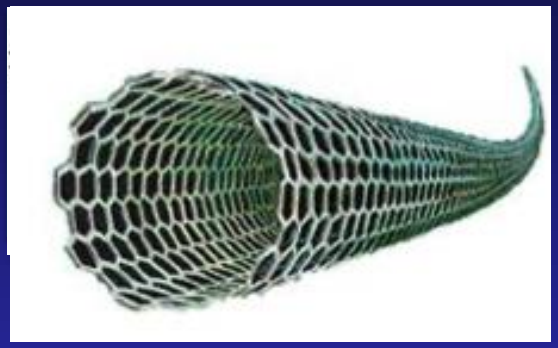

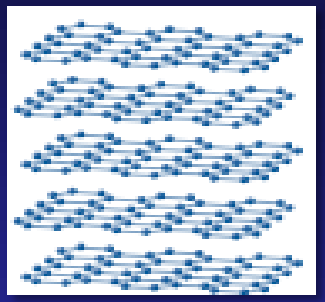

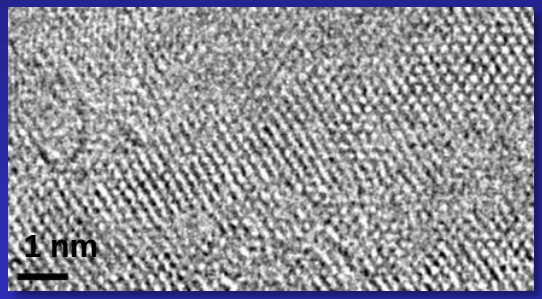

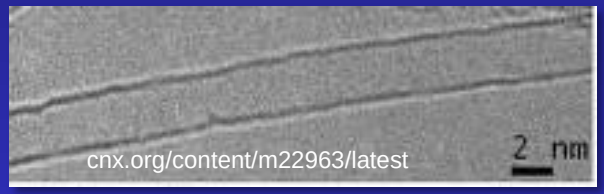

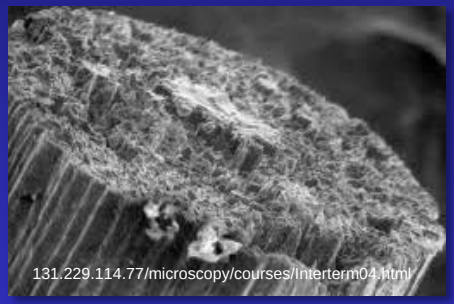

Graphene
2D confined material
Thermal conductivities
3080 to 5150 W/m/K in plane

J. C. Meyer, *et al. Nature.* 2007, 446
A. A. Balandin *et al*. *Nano Lett.* 2008, 8

Single Walled Carbon Nanotube
1D confined material
Thermal conductivities
2,500 to 10,000 W/m/K axial

C. H. Yu *et al. Nano Lett.*, **2005,** 5
E. Pop *et al. Nano Lett.*, **2006,** 6

Graphite
3D bulk material
Thermal conductivities
5.7 (⊥) to 1950 W/m/K (||)

Handbook of Chem. and Phys., 2010
B. T. Kelly, *Physics of Graphite,* 1981.

Thermopower wave: reaction wave pushes electrons

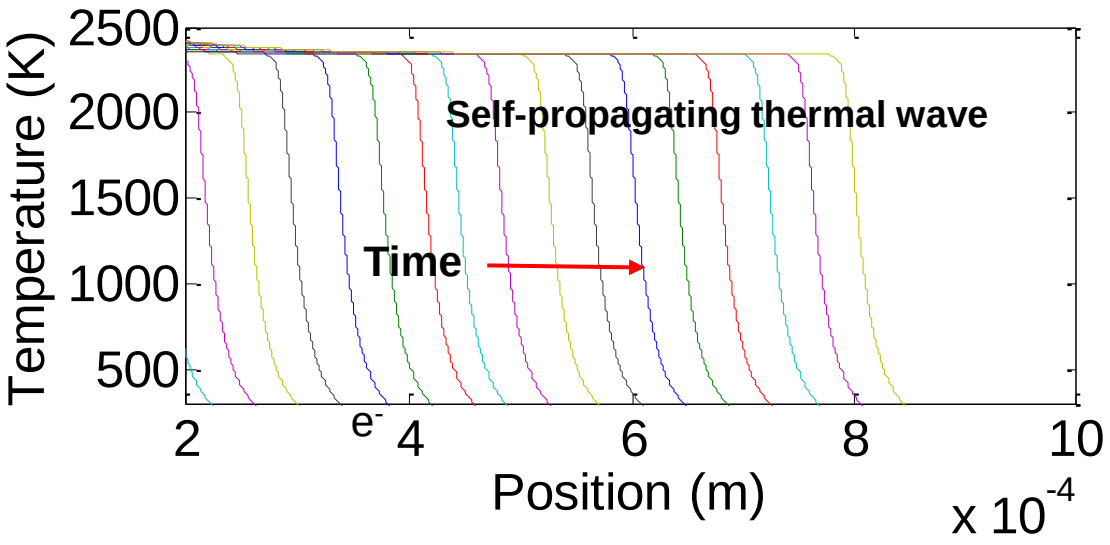

Heat transfer from nanowire to fuel

Fuel

enthalpy of reaction

Molar density of fuel (1st order decomposition)

$$\frac{\rho C_p}{M_W}\frac{\partial T}{\partial t} = \chi\frac{\partial^2 T}{\partial x^2} + Q\left(\frac{\partial y}{\partial t}\right) - G\left(T - T_2\right)$$

Energy balance for fuel

molar weight

thermal conductivity

interfacial conductivity

$$\frac{\rho_2 C_{p,2}}{M_{W2}}\frac{\partial T_2}{\partial t} = \chi_2\frac{\partial^2 T_2}{\partial x^2} + G\left(T - T_2\right)$$

Energy balance for thermal conduit

Abrahamson JT and Strano MS, J. Phys. Chem. Letters, 1 (2010) 3514–3519

Chemically driven thermal waves along CNT

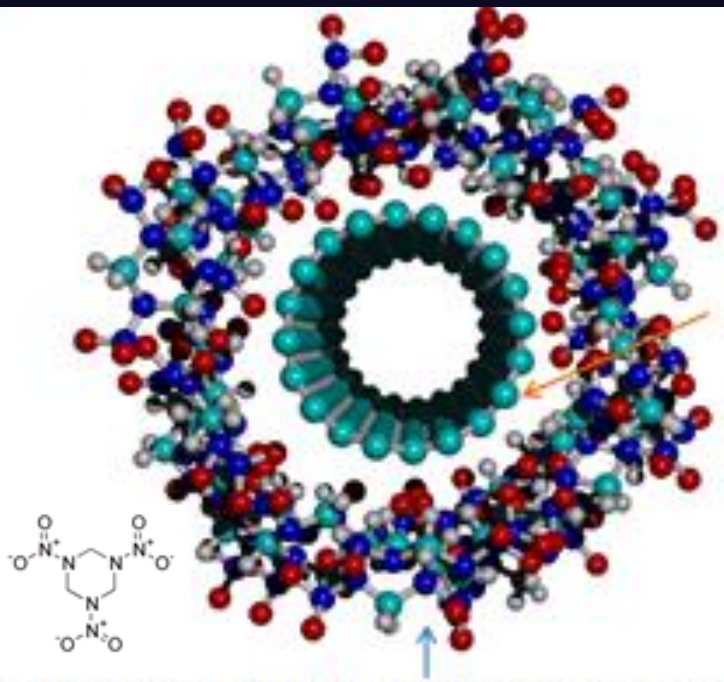

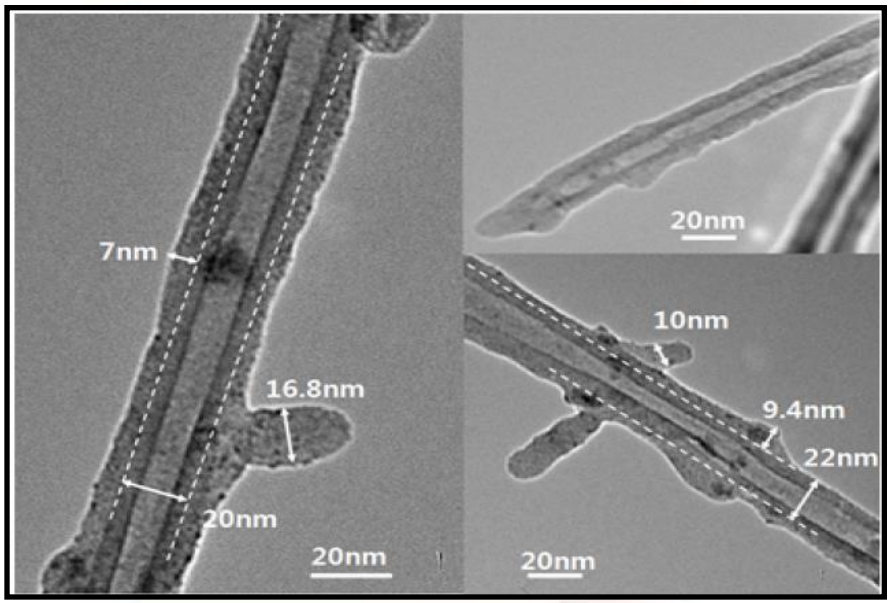

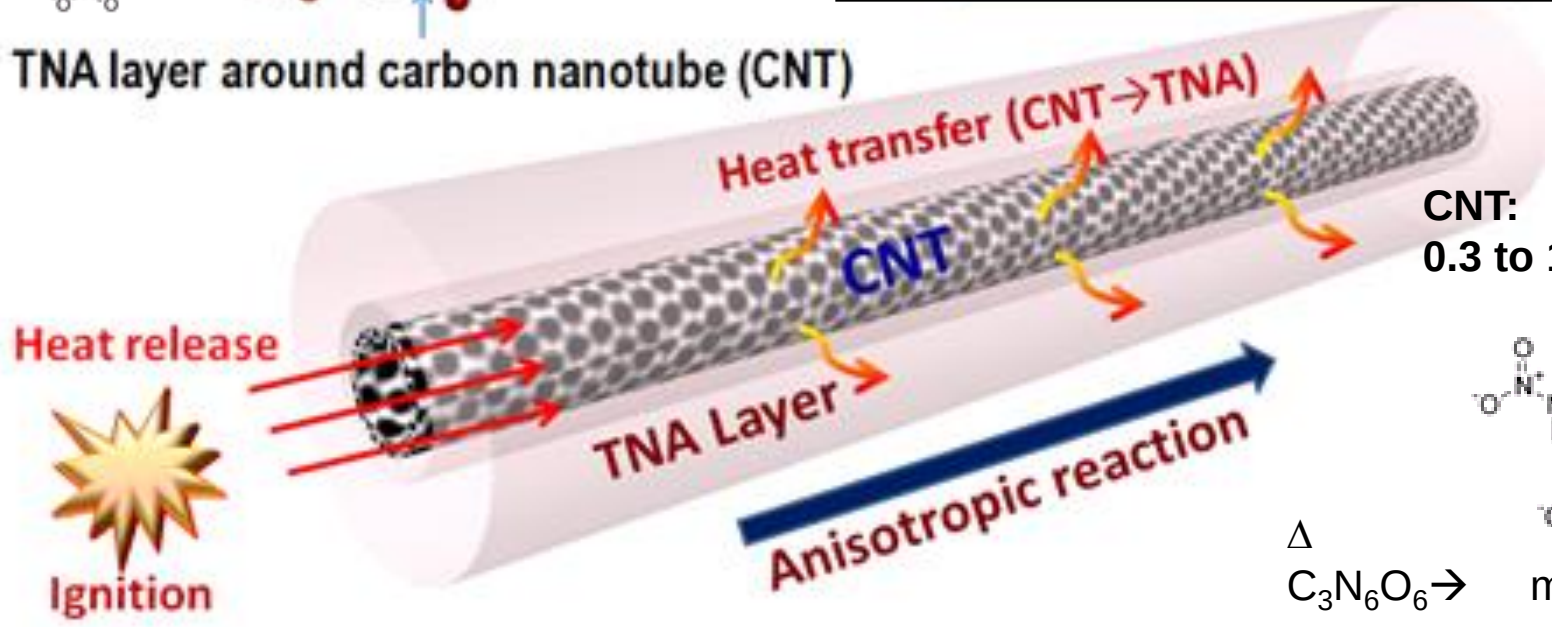

CNT:
0.3 to 10 kW/m/K

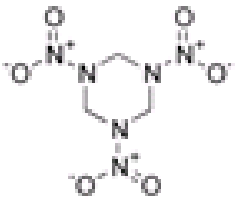

Δ
$C_3N_6O_6 \rightarrow$ more Δ

W Choi, S Hong, JT Abrahamson *et al*. *Nature Materials*, 9, **2010**, 423

Thermopower Waves in Carbon Yarns

Carbon nanotubes can be spun into **yarns**, and coated with organic fuel (trinitroamine)

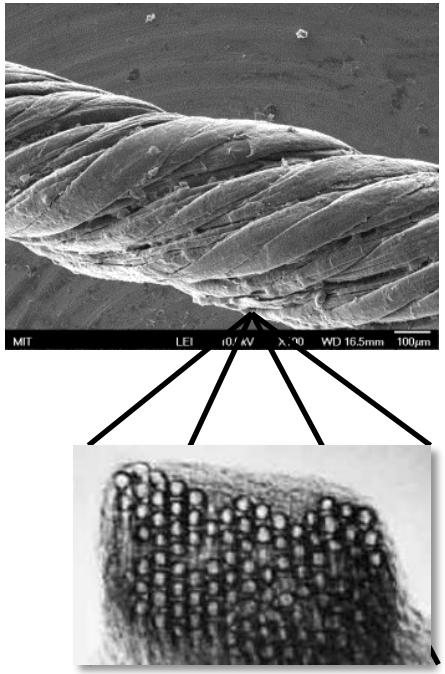

Choi W, Abrahamson JT, Strano JM, Strano MS: Materials Today, 13 (2010) 22-33

1D thermal wave is accelerated x10000

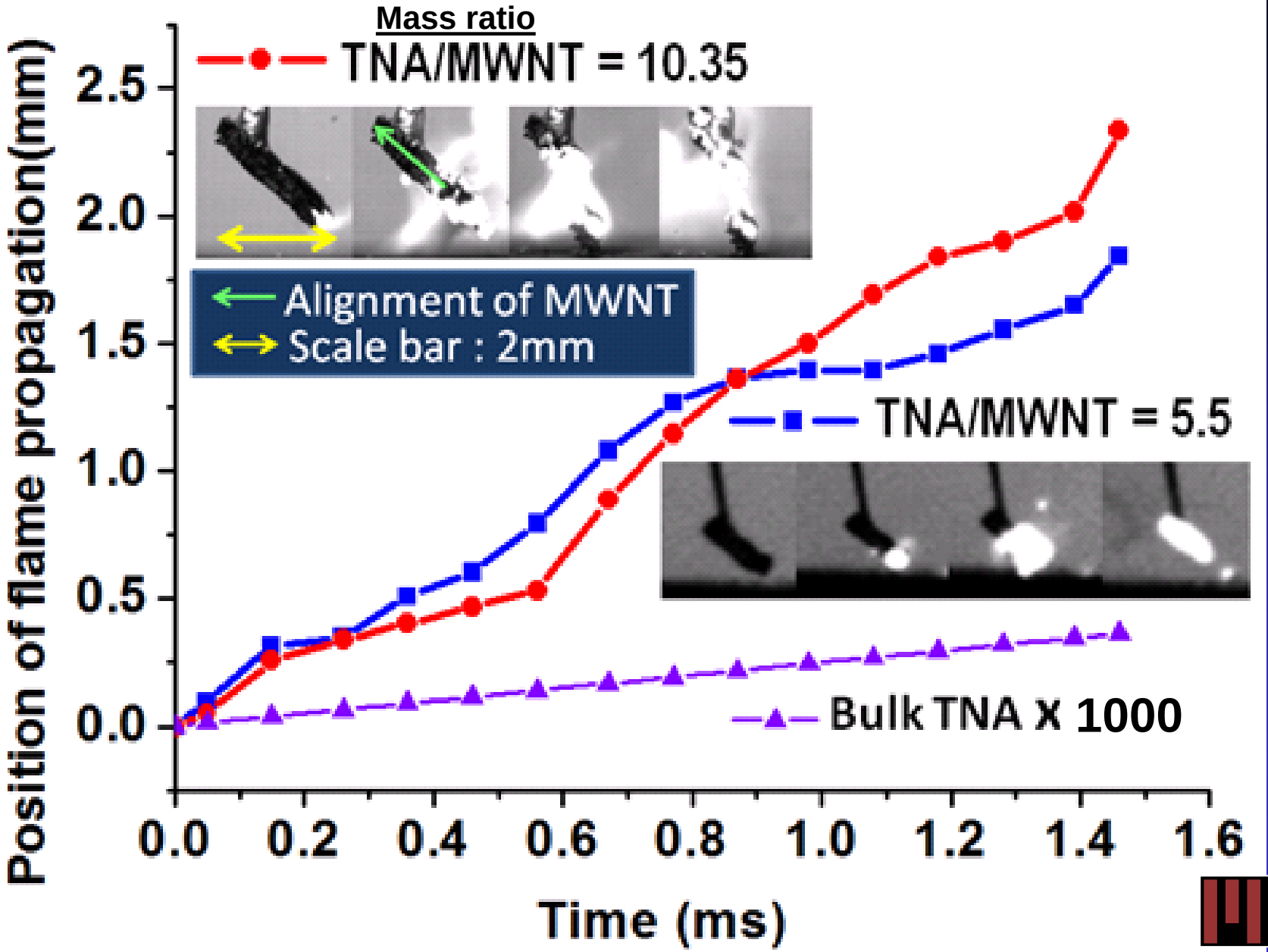

W Choi, S Hong, JT Abrahamson *et al*. *Nature Materials*, 9, **2010**, 423

Reaction induces an electrical pulse:
thermopower wave – a first demonstration

Electrons entrained in the thermal wave drive a current along nanotube

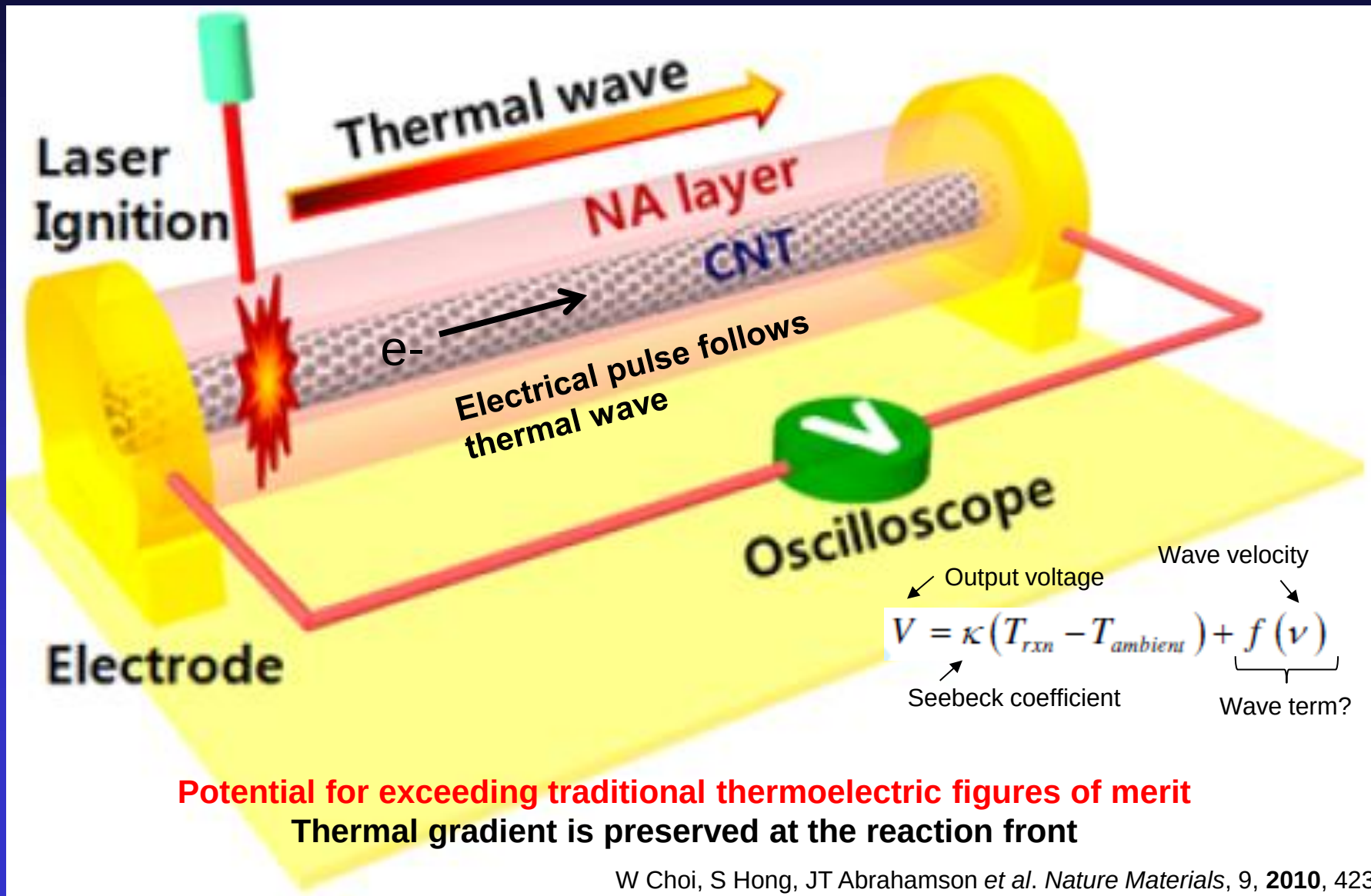

Potential for exceeding traditional thermoelectric figures of merit

Thermal gradient is preserved at the reaction front

W Choi, S Hong, JT Abrahamson *et al*. *Nature Materials*, 9, **2010**, 423

Thermopower electrical pulse follows thermal wave propagation

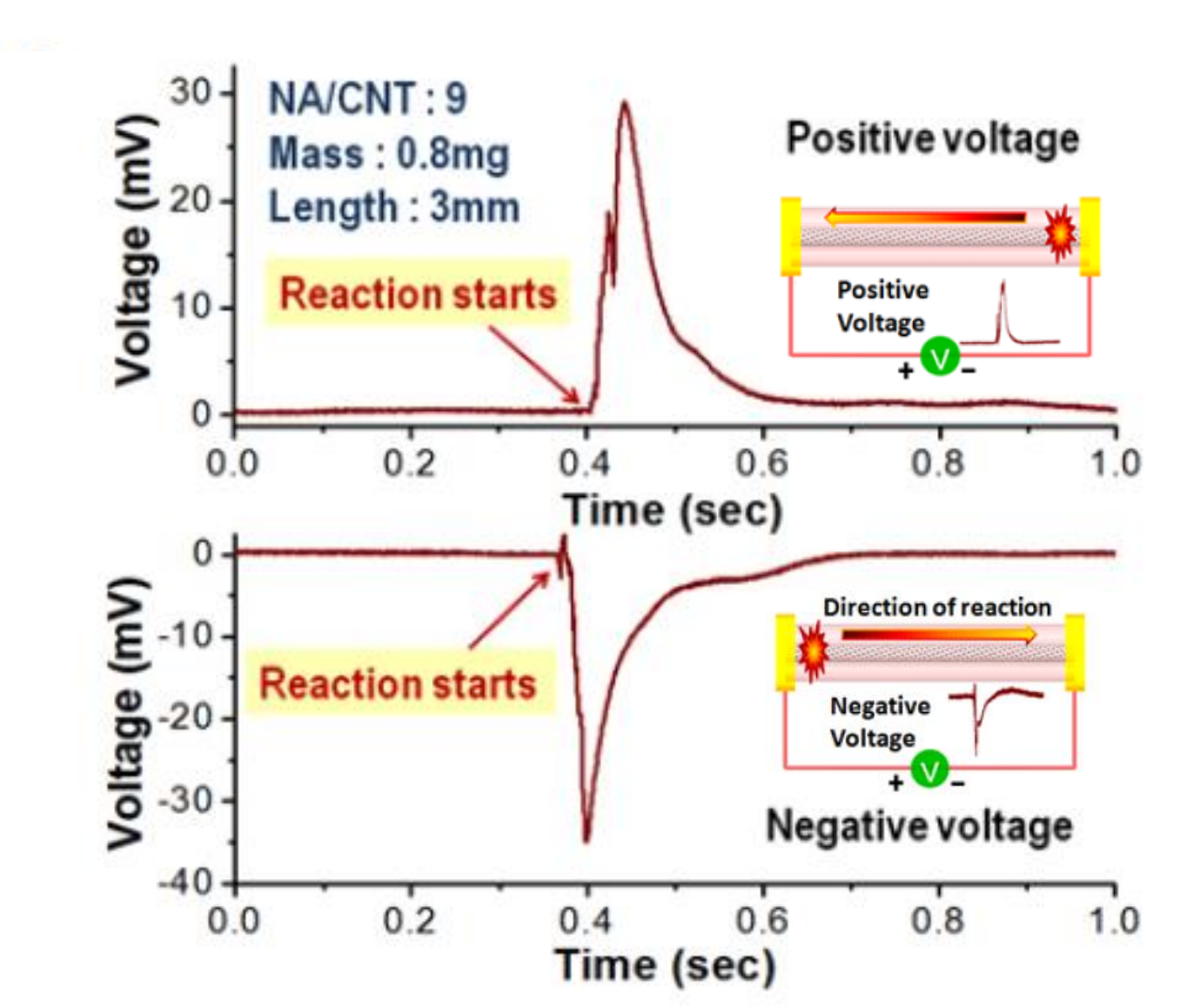

W Choi, S Hong, JT Abrahamson *et al*. *Nature Materials*, 9, **2010**, 423

Slow Wave Velocities Yield Conventional Thermopower

Output voltage

Wave velocity

$$V = \kappa\left(T_{rxn} - T_{ambient}\right) + f\left(v\right)$$

Seebeck coefficient

Wave term?

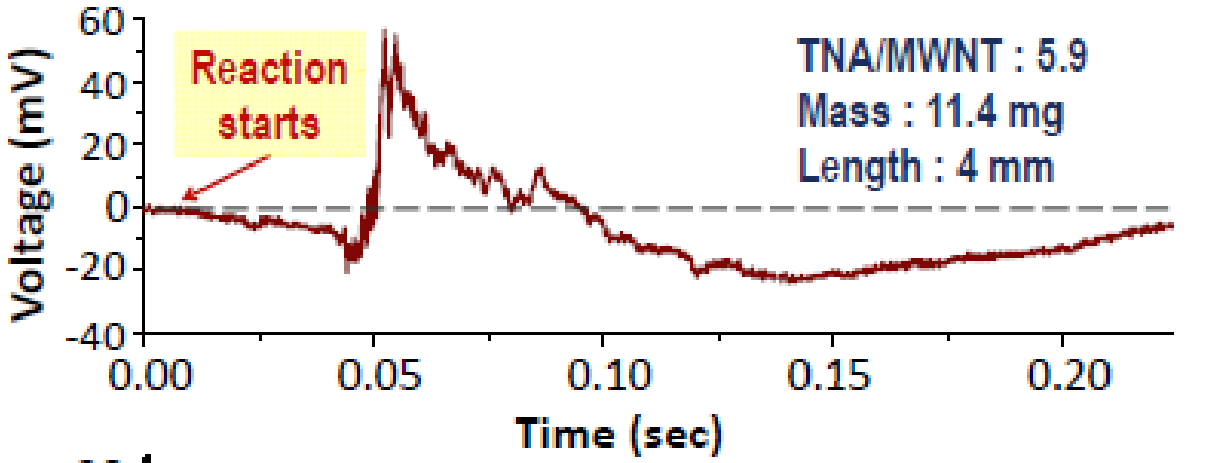

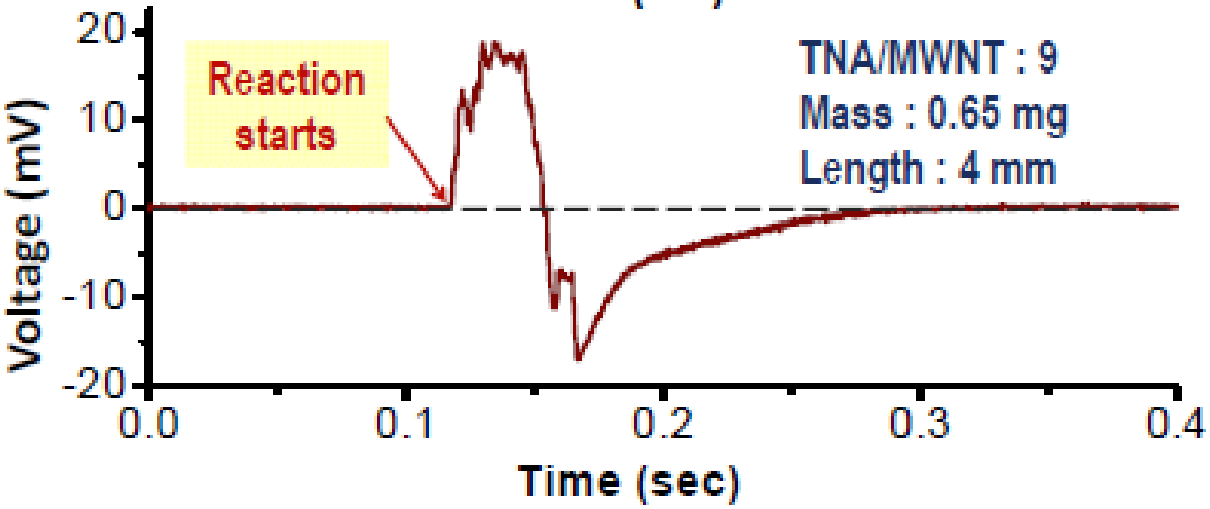

Conventional thermopower (a slow wave) yields a sinusoidal voltage profile as the reaction zone traverses the nanotube

W Choi, S Hong, JT Abrahamson *et al*. *Nature Materials*, 9, **2010**, 423

Thermopower Wave Research at MIT

Courtesy: The Discovery Channel

Temperature, Voltage and Visual Sync

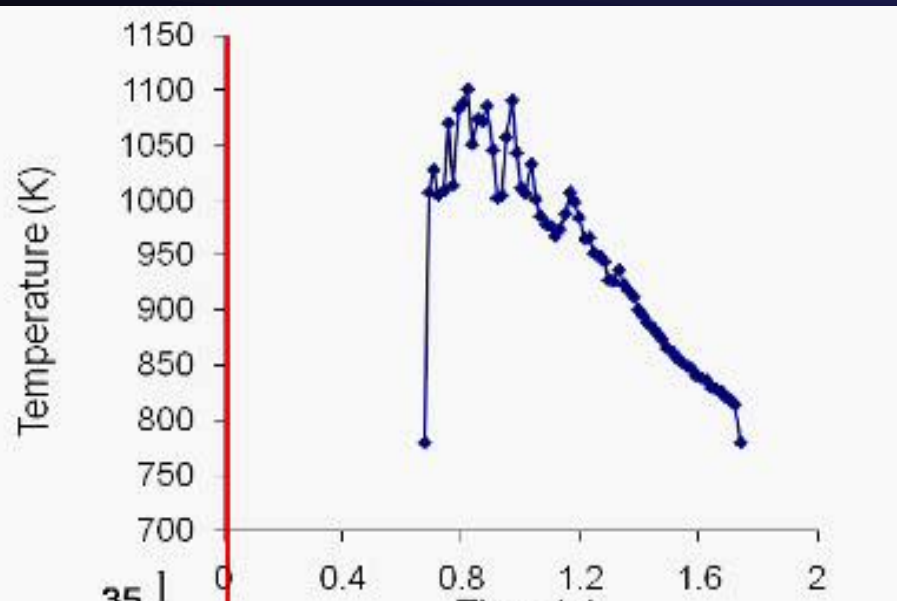

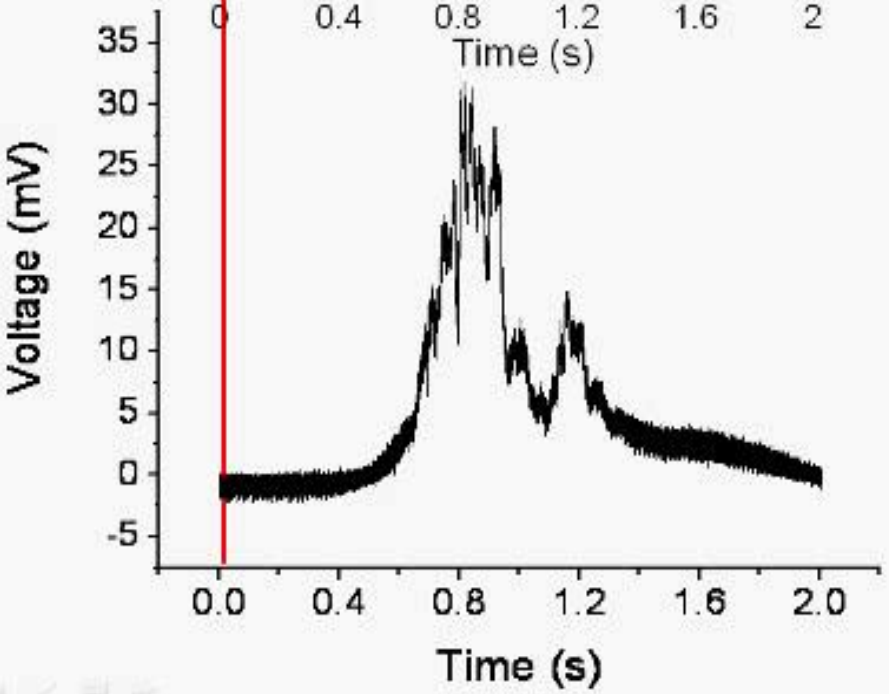

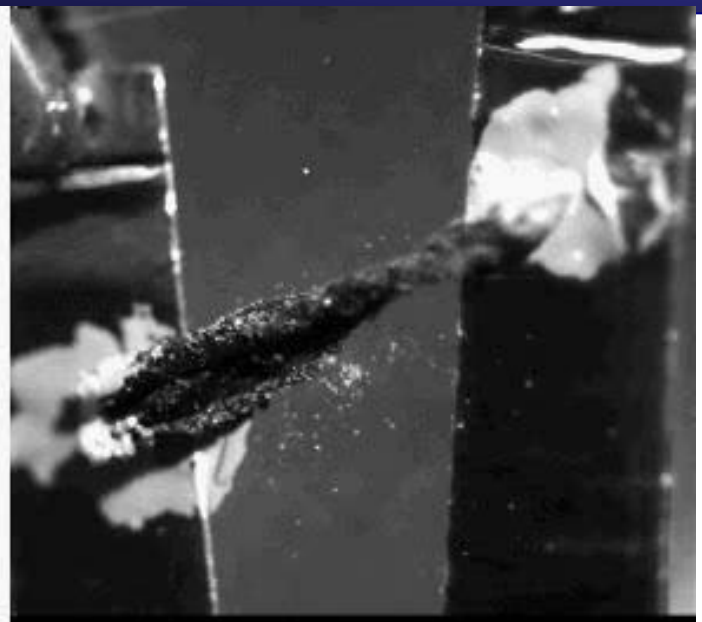

The carbon <u>survives</u> the high temperature and can be used again!

Theoretical Calculations Predict Oscillating Thermal Wavefronts: AC Batteries

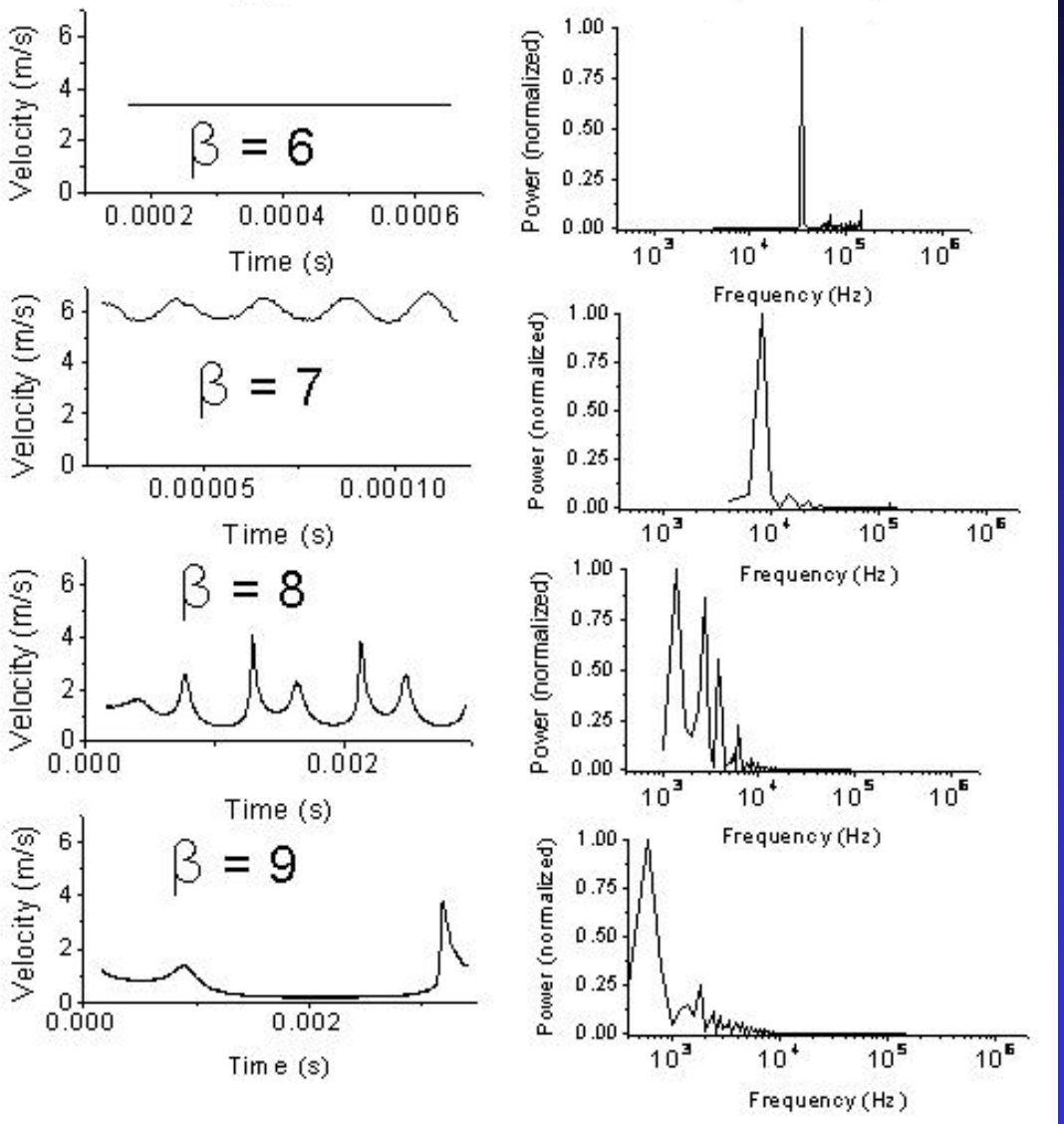

Activation energy

Heat capacity

Inverse adiabatic reaction temperature

$$\beta = \frac{C_p E_a}{-QR}$$

Heat of reaction

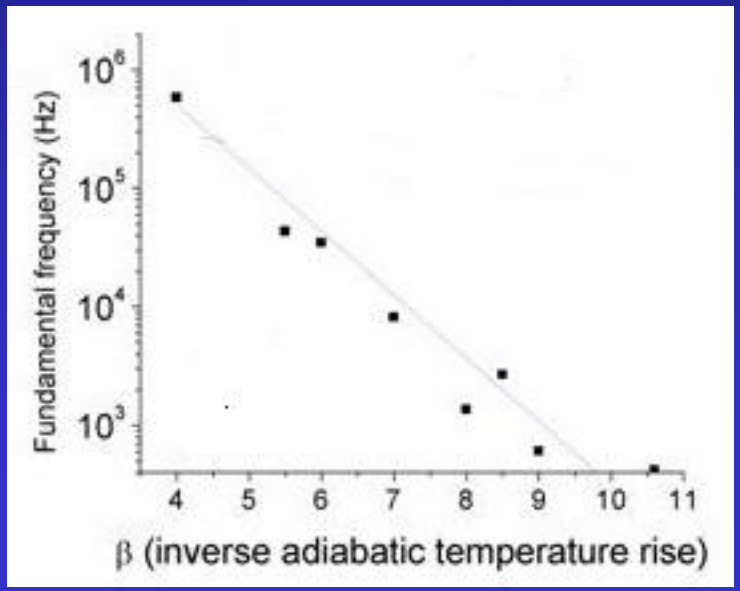

Abrahamson, J., et al ACS Nano (2010)

New Concepts in Mass and Energy Transport within Carbon Nanotubes

- Coherence resonance in molecular transport through a single walled carbon nanotube nanopore

- Energy storage and generation using thermopower waves

- Near infrared fluorescent sensors with single molecule sensitivity for studying biological signaling fluxes: reactive oxygen and nitric oxide signaling in Epidermal Growth Factor Receptor (EGFR)

Optical Properties: Near Infrared Band Gap

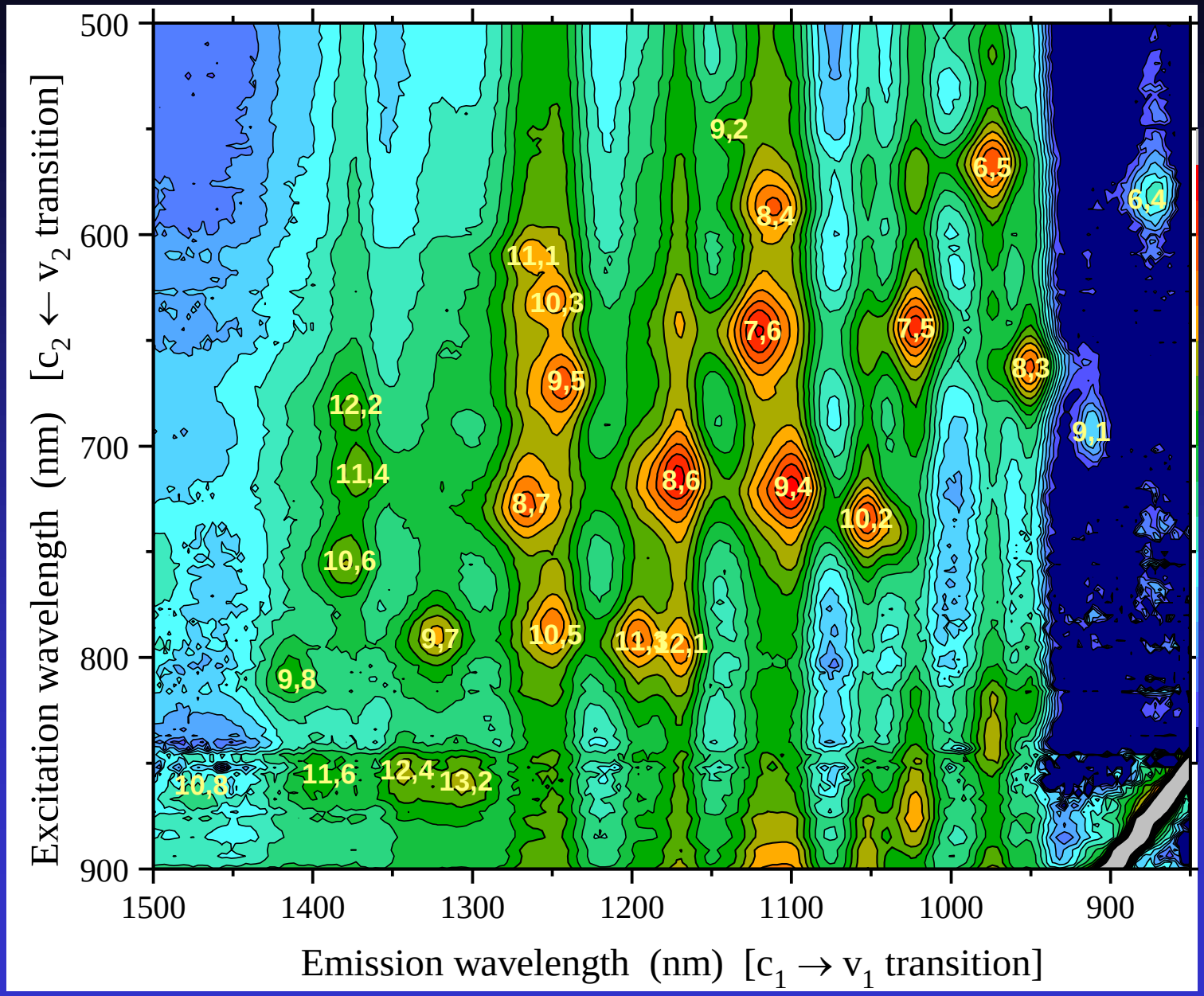

Bachillo, S., Strano, M. S. et al., *Science, 298 (2002) 2361*

Semiconducting Carbon Nanotubes Fluoresce

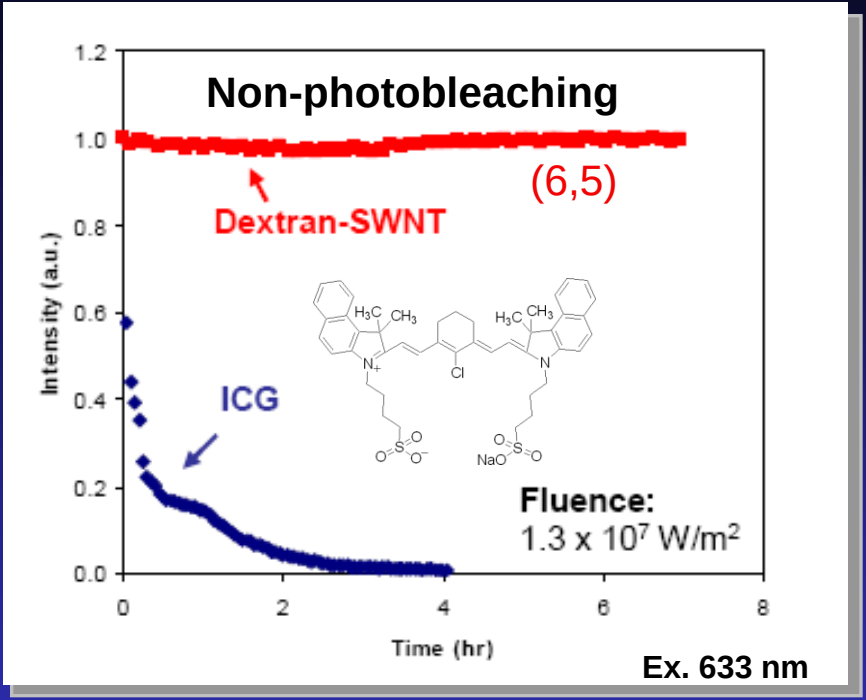

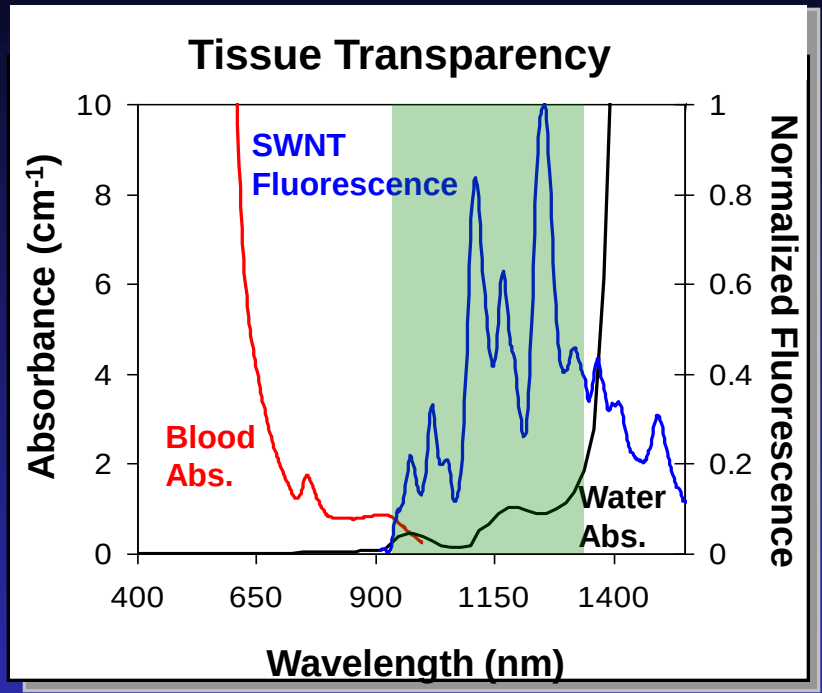

SWNT are non-photo-bleaching, no blinking at high fluence

Near infrared emission is uniquely situated in the *tissue transparency window*; no auto-fluorescence from biomaterials

No surface states, environmentally sensitive (two types):

Solvatochromism (emission wavelength changes)

Charge transfer, quenching (intensity variation)

Single Molecule Detection using SWNT Fluorescence

1D confined exciton can detect stochastic adsorption of single molecules

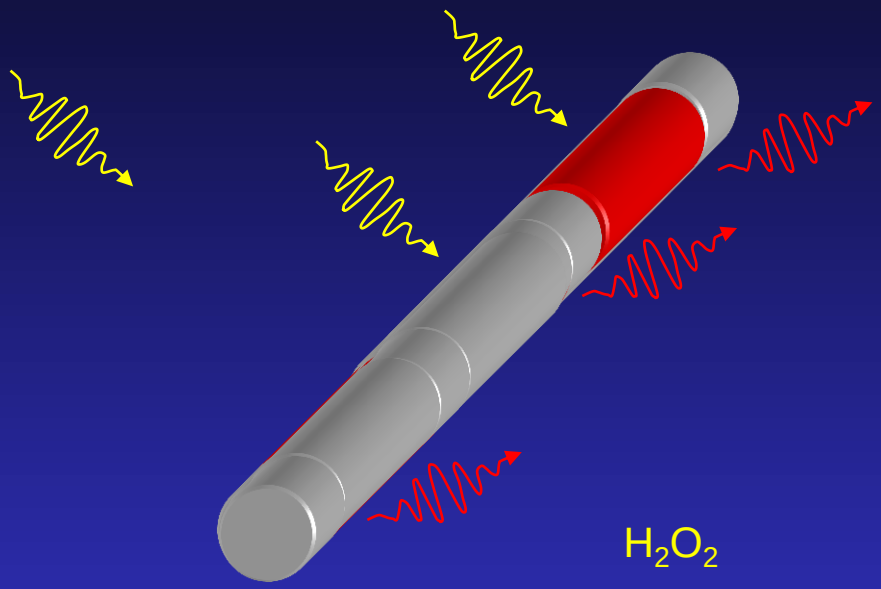

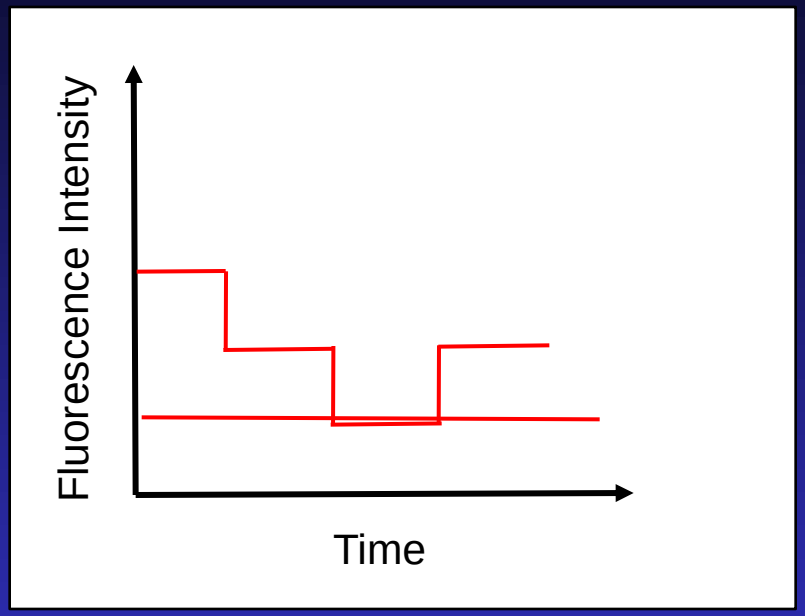

H_2O_2

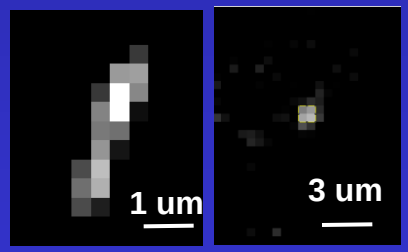

Long SWNT

Typical SWNT

Exciton excursion distance = 90 nm **Cognet et al** *Science* ***316, 1465-1468 (2007)***

In diffraction limited spot, as many as 900 nm/ 90 nm ~ 10 emission states (3 shown above)

Quenching molecules (NO, H_2O_2, H^+, $Fe(CN)_6^{3-}$) extinguish emission of state stochastically

Jin et al. *Nanoletters* **8 (12) 4299-4304 (2008)**

Single Molecule Detection In-Vivo using a Collagen Platform

Hong Jin

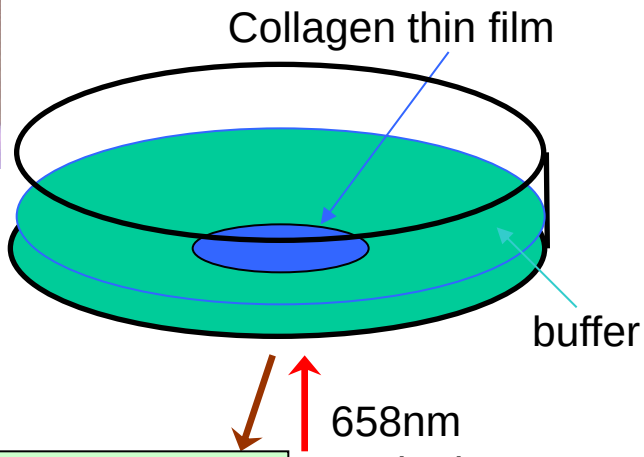

SWNT embedded into type 1 collagen film

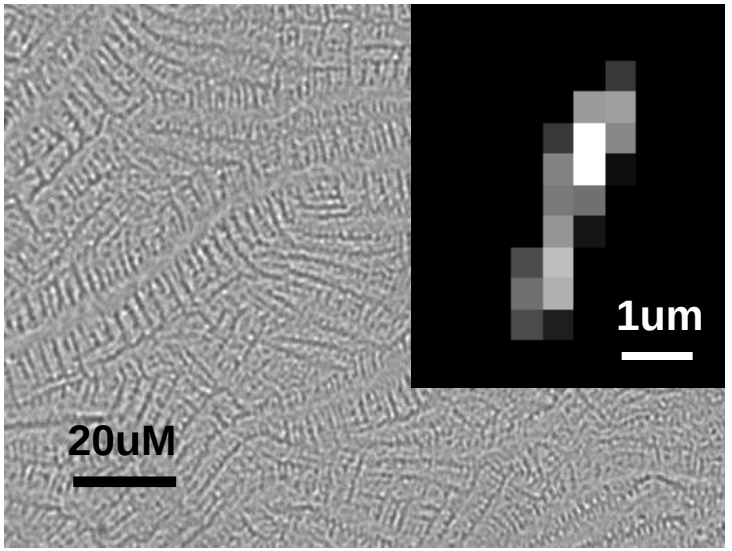

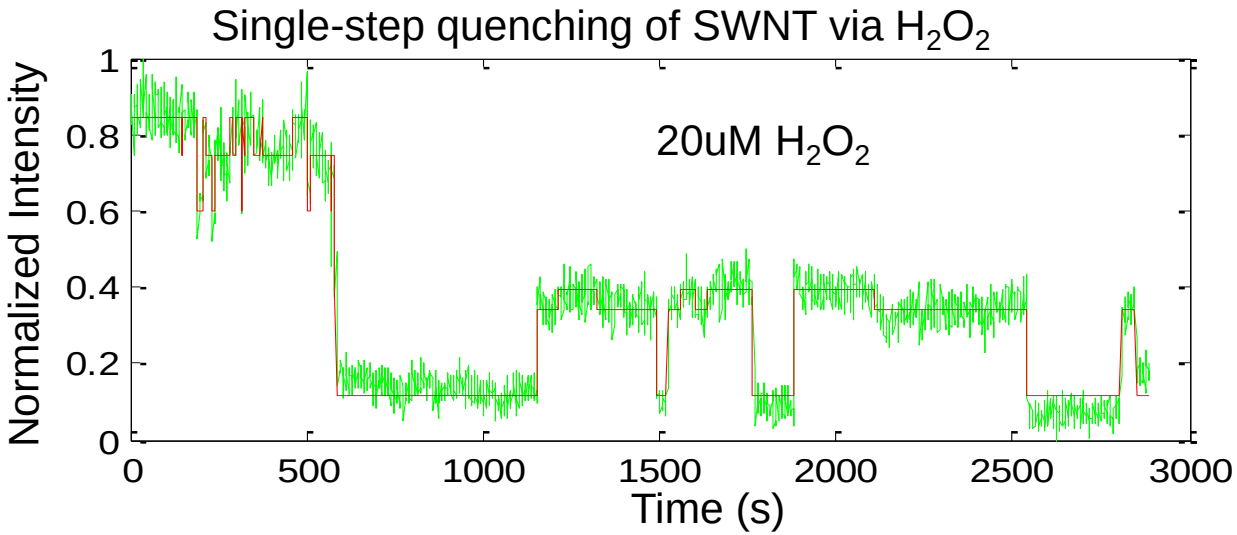

Red line: fit to Hidden Markov model

McKinney, S. A.; Joo, C.; Ha, T. *Biophysical Journal* **2006**, *91*, 1941-1951.

H Jin, et al. Nanoletters 8 (12) 4299-4304 (2008)

Single Molecule Detection of Hydrogen Peroxide

InGaAs nIR Detector
(0.7 to 1.9 um)

Objective:
1.46 NA (TIR)

Single isolated SWNT in collagen film, 10 uM H_2O_2

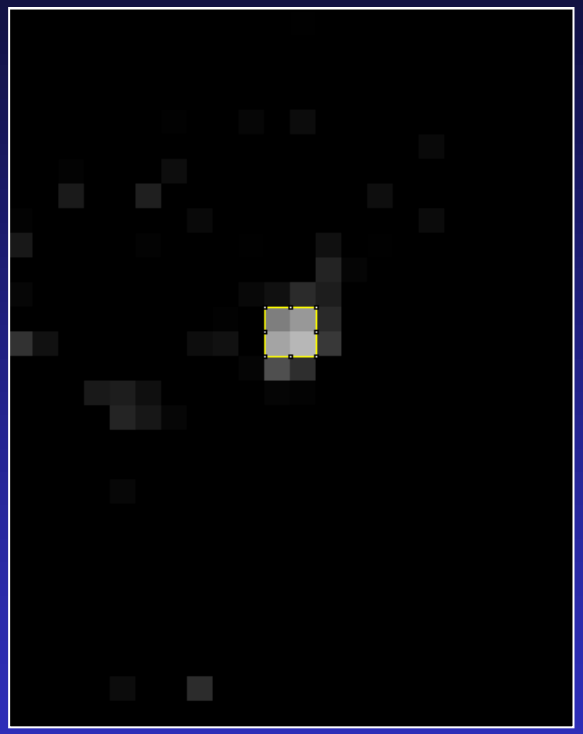

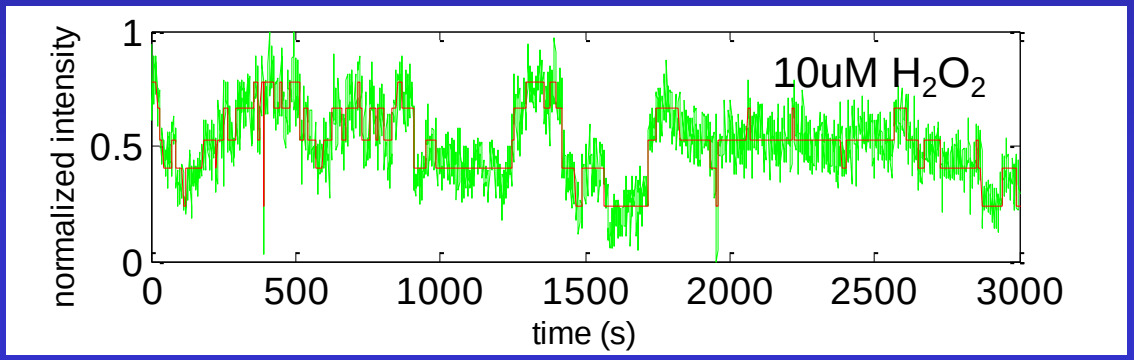

H Jin, et al. Nanoletters 8 (12) 4299-4304 (2008)

Biological Problem: Epidermal Growth Factor Receptor

Epidermal Growth Factor Receptor (EGF): extracellular membrane protein; tyrosine kinase; ErbB family of receptors; modulates cell proliferation

EGFR over-expression implicated in many cancers.

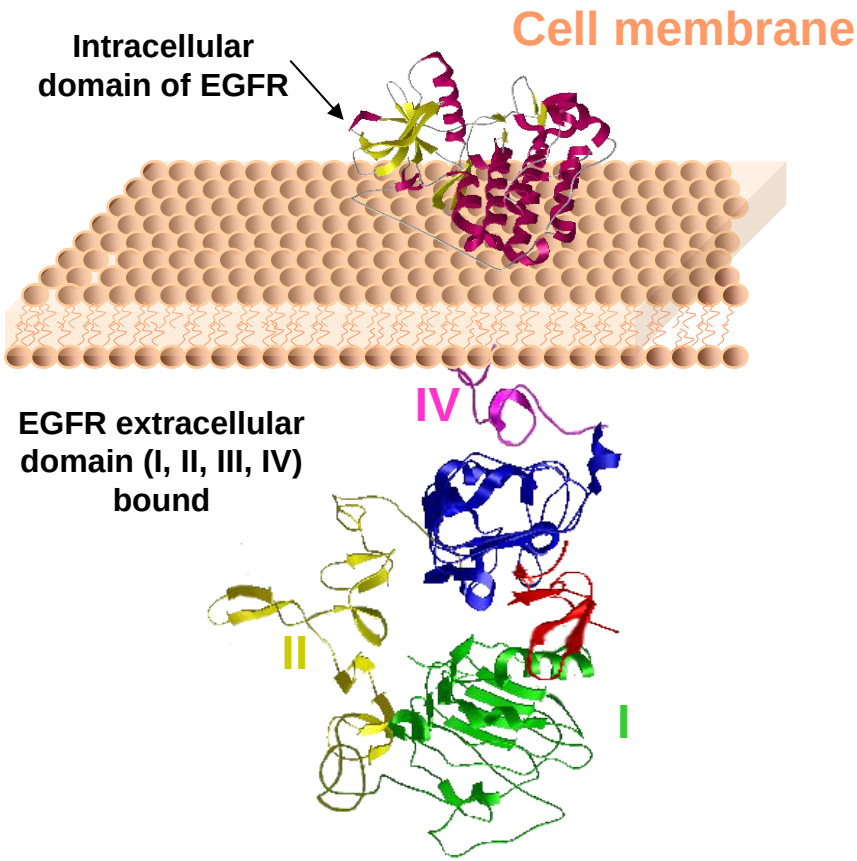

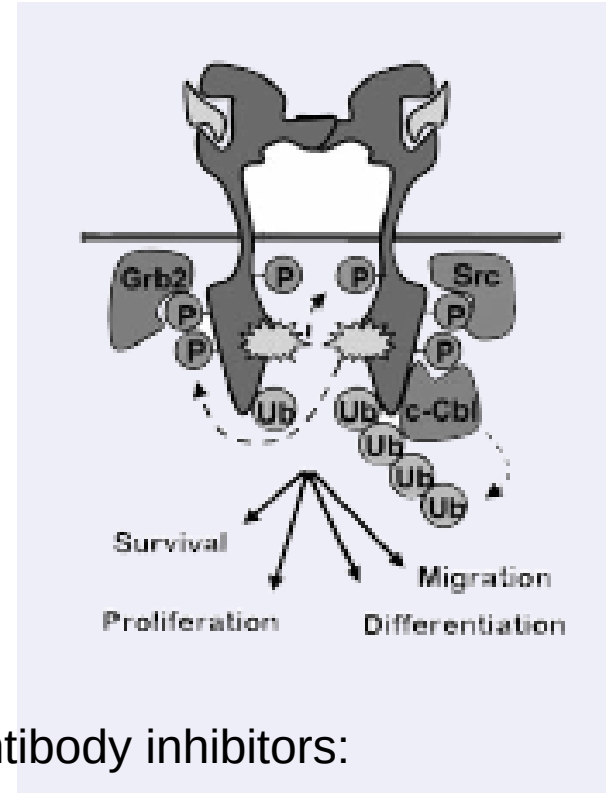

Monoclonal antibody inhibitors:

Cetuximab and Panitumumab

> $620 million/year

Grandal et al. *J. Cell. Mol. Med. Vol 12, No 5A, 2008 pp. 1527-1534*

Questions about H_2O_2 signaling pathway in EGFR

Source of H_2O_2 generation in response to EGF stimulation
Location within the cell
Relationship to better known phosphorylation pathway

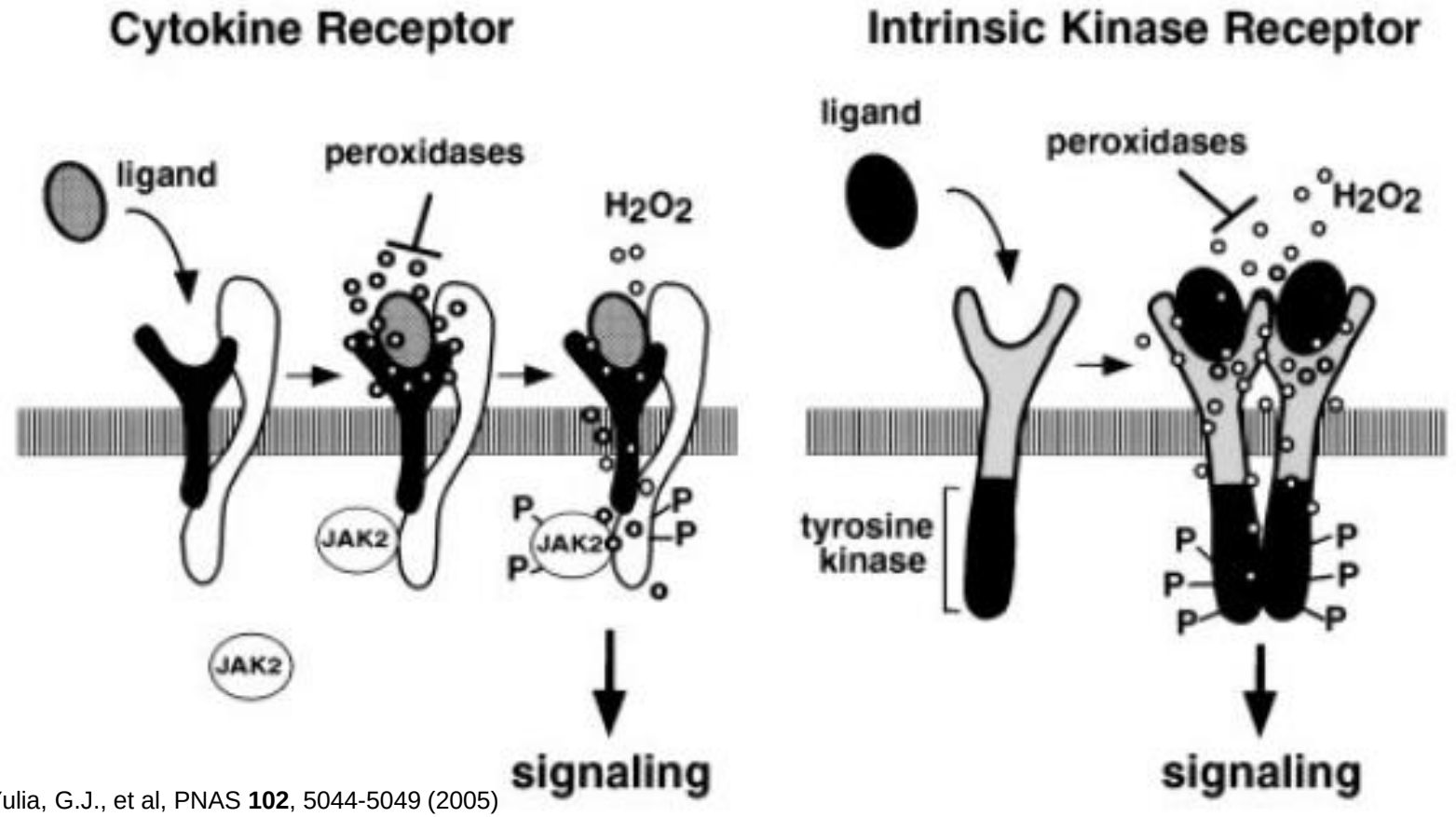

DeYulia, G.J., et al, PNAS **102**, 5044-5049 (2005)

Goal of our work: develop a platform to study ROS signaling at the single cell, single molecule level

Spatial and Temporal Single Molecule Map from Live A431 Human Epidermoid Carcinoma

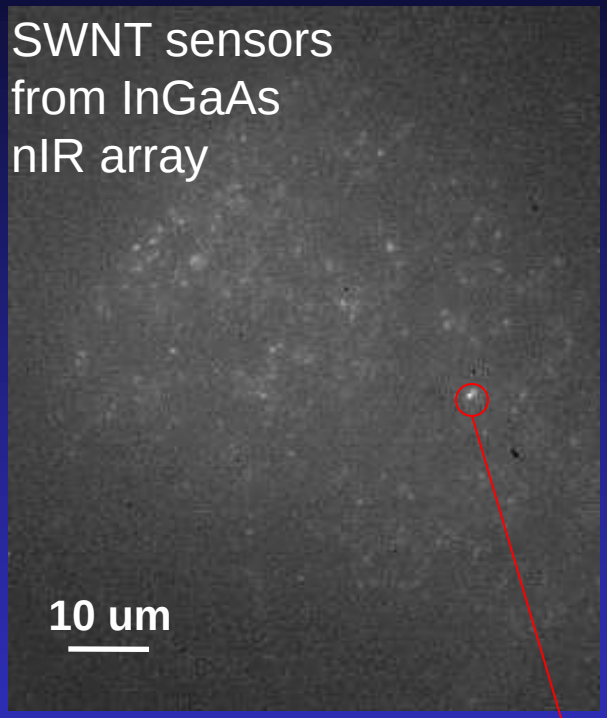

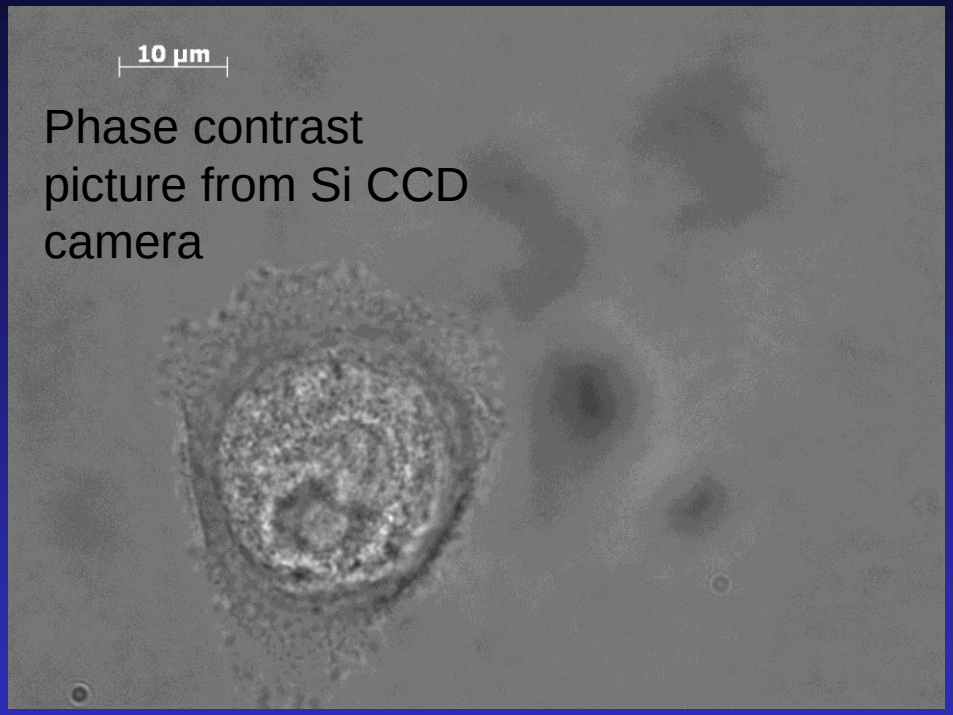

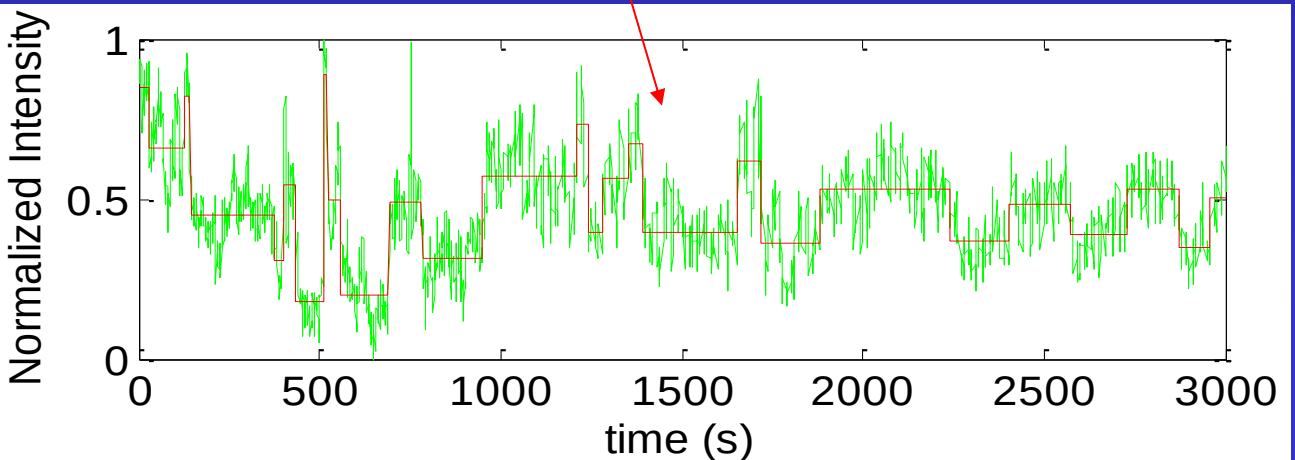

One example trace, from a 4 pixel region of interest (ROI) on one single nanotube.

The goal is to examine all the ROIs and map the spatial behavior in real time.

Real Time, Spatially Resolved Single Molecule Detection of H_2O_2 from a single A431 Cell

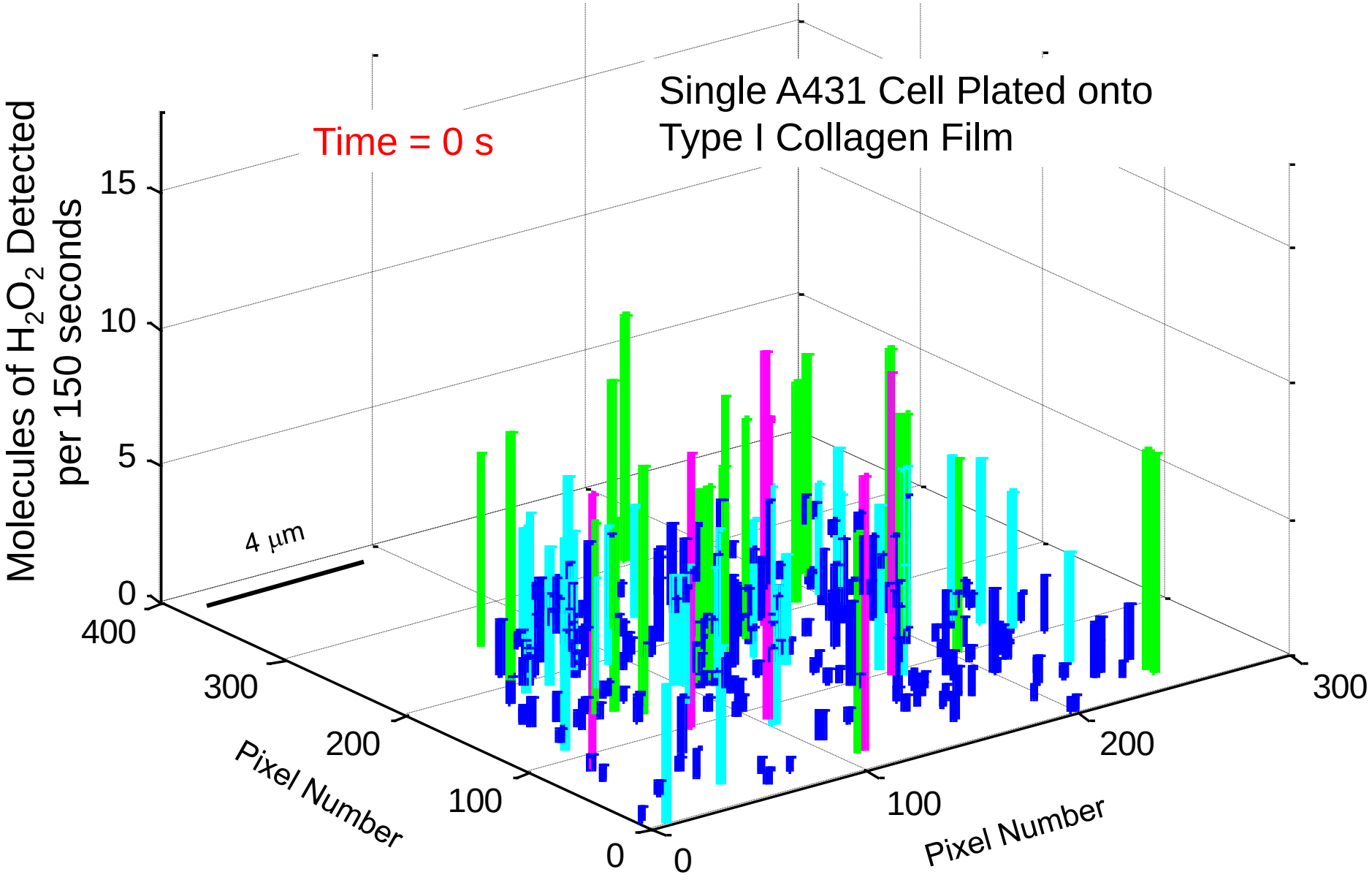

Real Time, Spatially Resolved Single Molecule Detection of H_2O_2 from a single A431 Cell

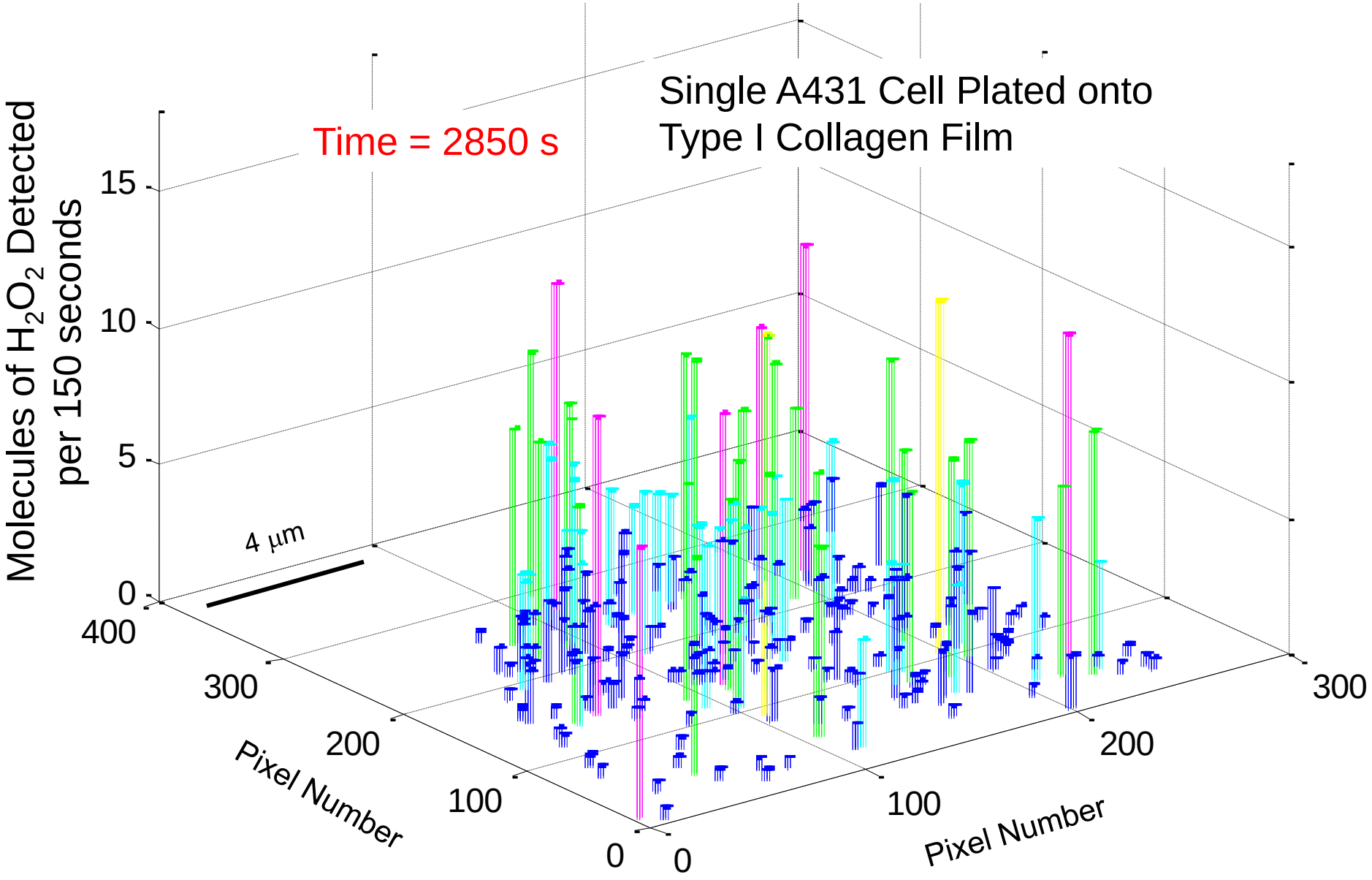

Single cell analysis

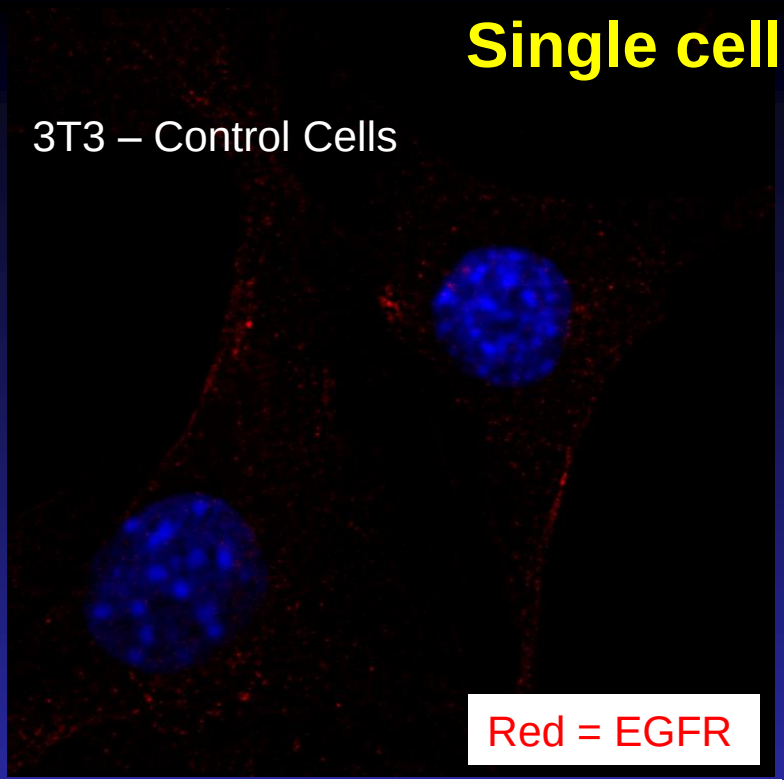

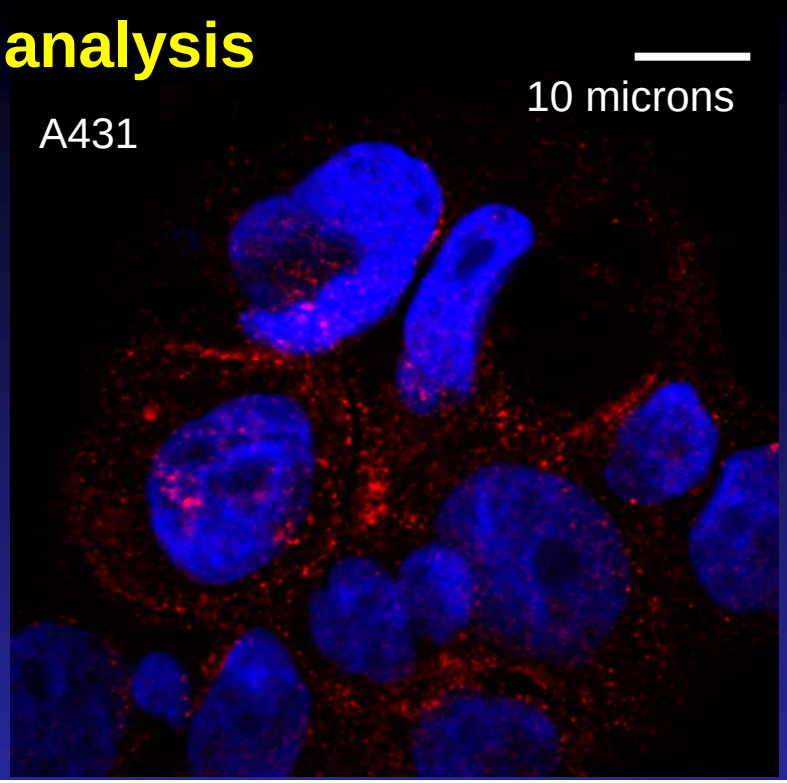

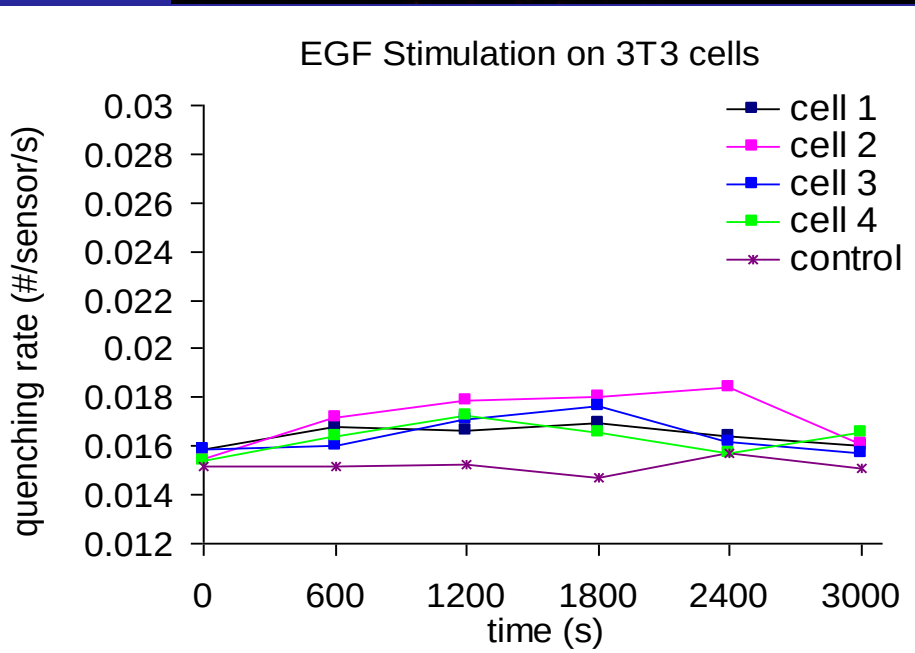

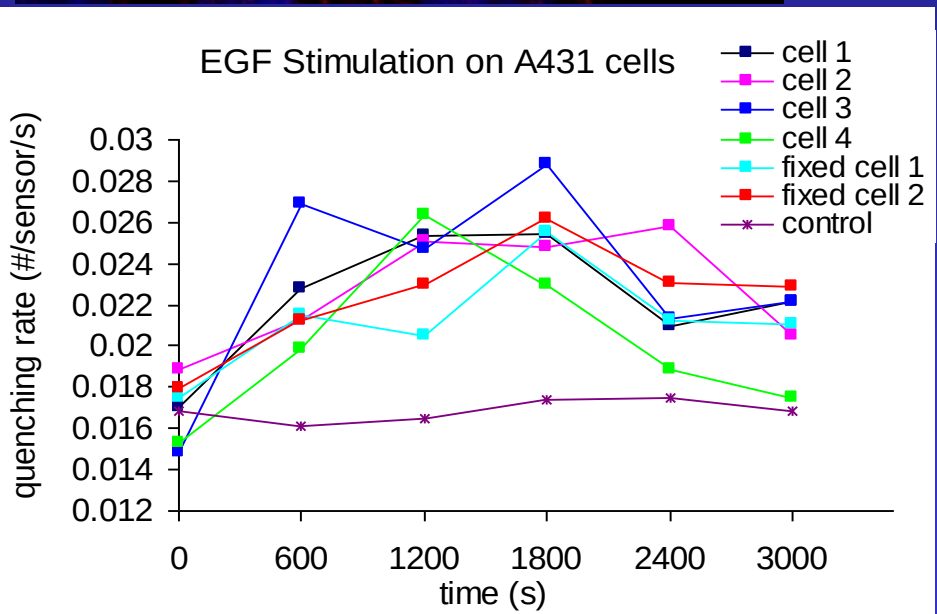

Sensors can distinguish background/membrane generation!

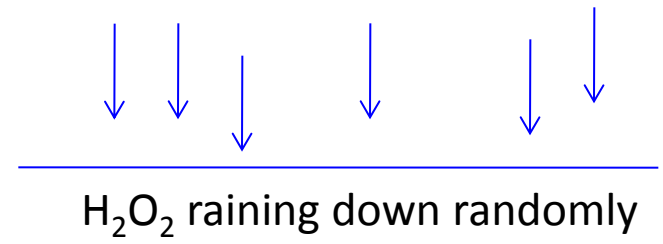

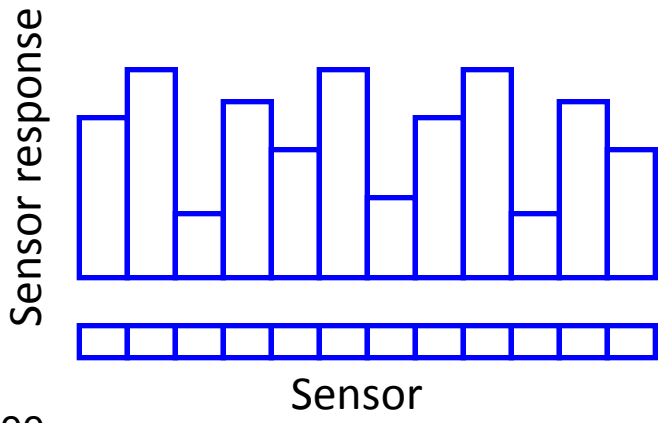

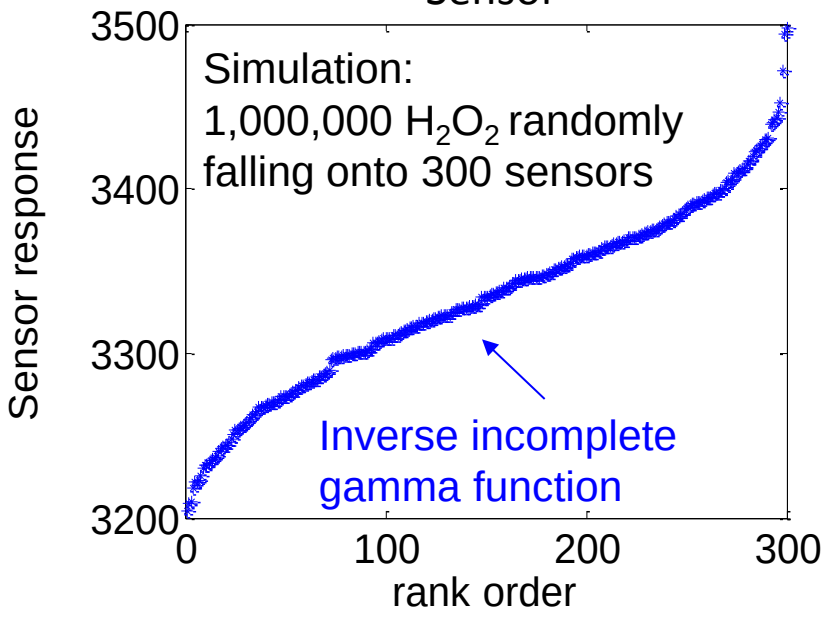

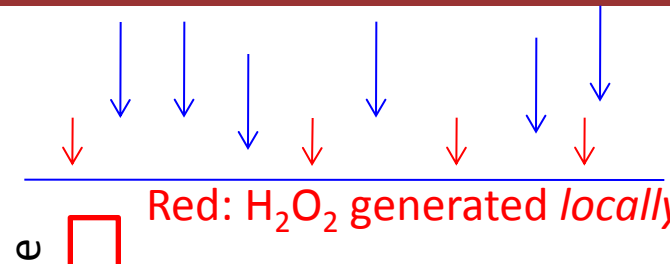

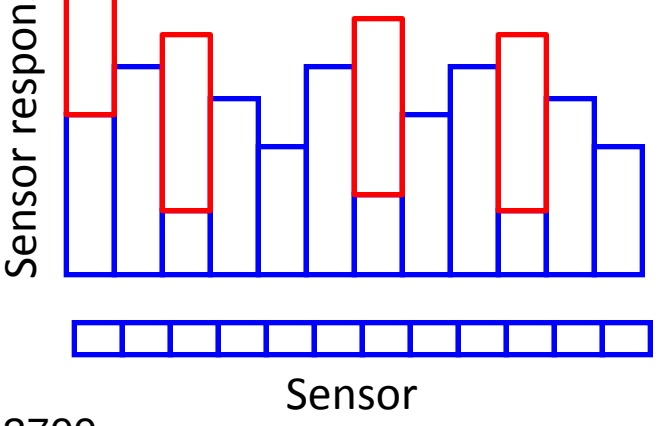

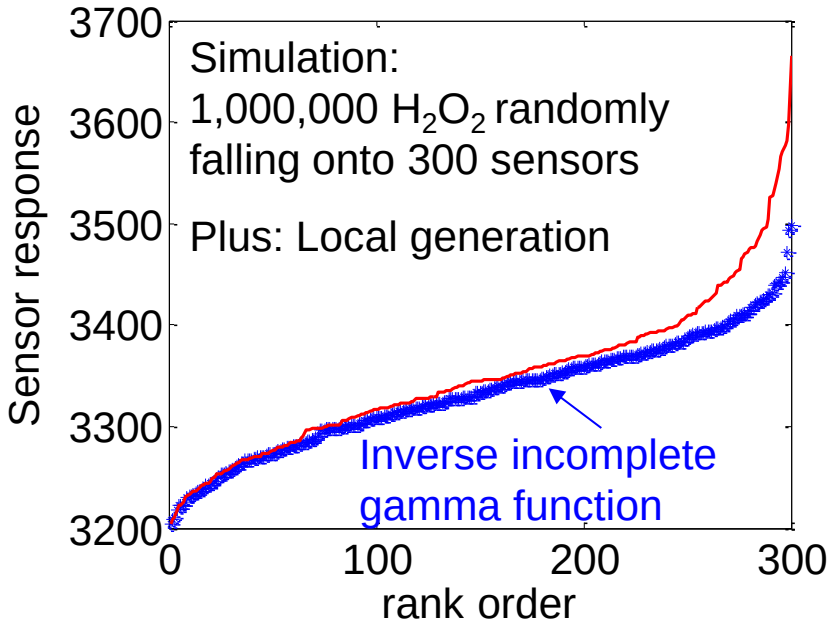

Counting molecules originating from the membrane

Given any distribution of sensor responses (rank ordered), y(x), the curve at $x \rightarrow 0$ specifies the binomial background (gamma function):

$$y_{membrane}(x) = y(x) - \Gamma\left(p, \frac{x}{n}\right)$$

Γ: incomplete gamma function (background)

p: mean value of background distribution, obtained from fitting the small number of data points at $x \rightarrow 0$

n = number of sensors

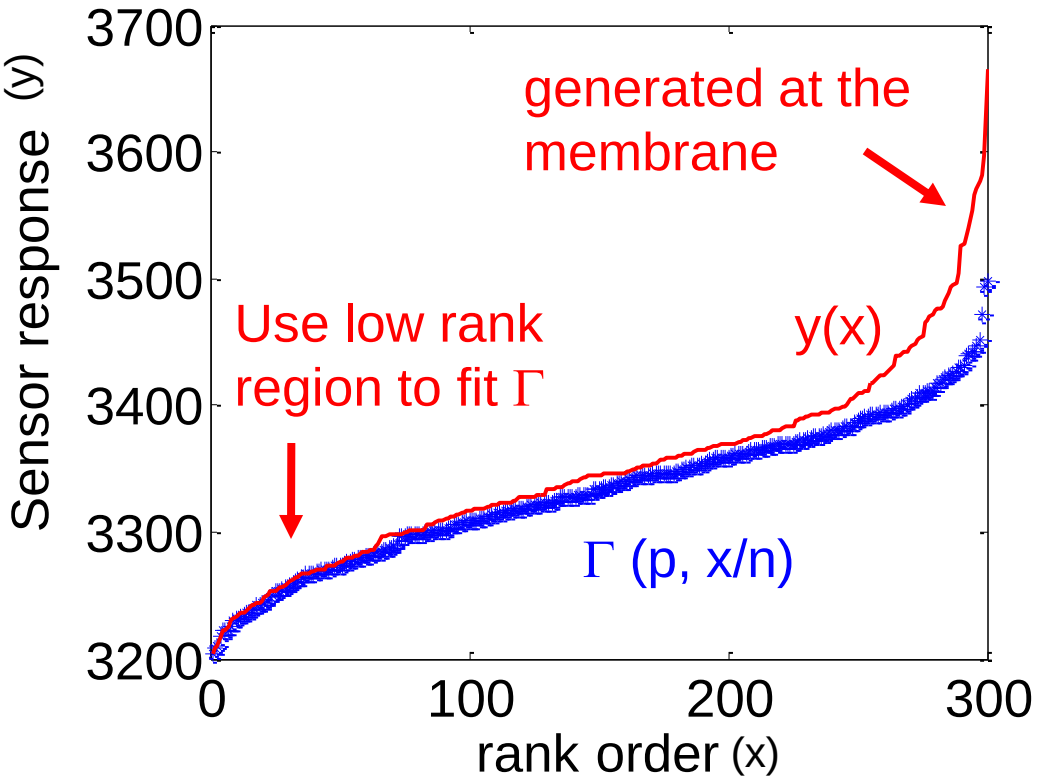

Jin, H., et al, Nature Nanotechnology (2010)

Separating EGFR Effect From Background H_2O_2

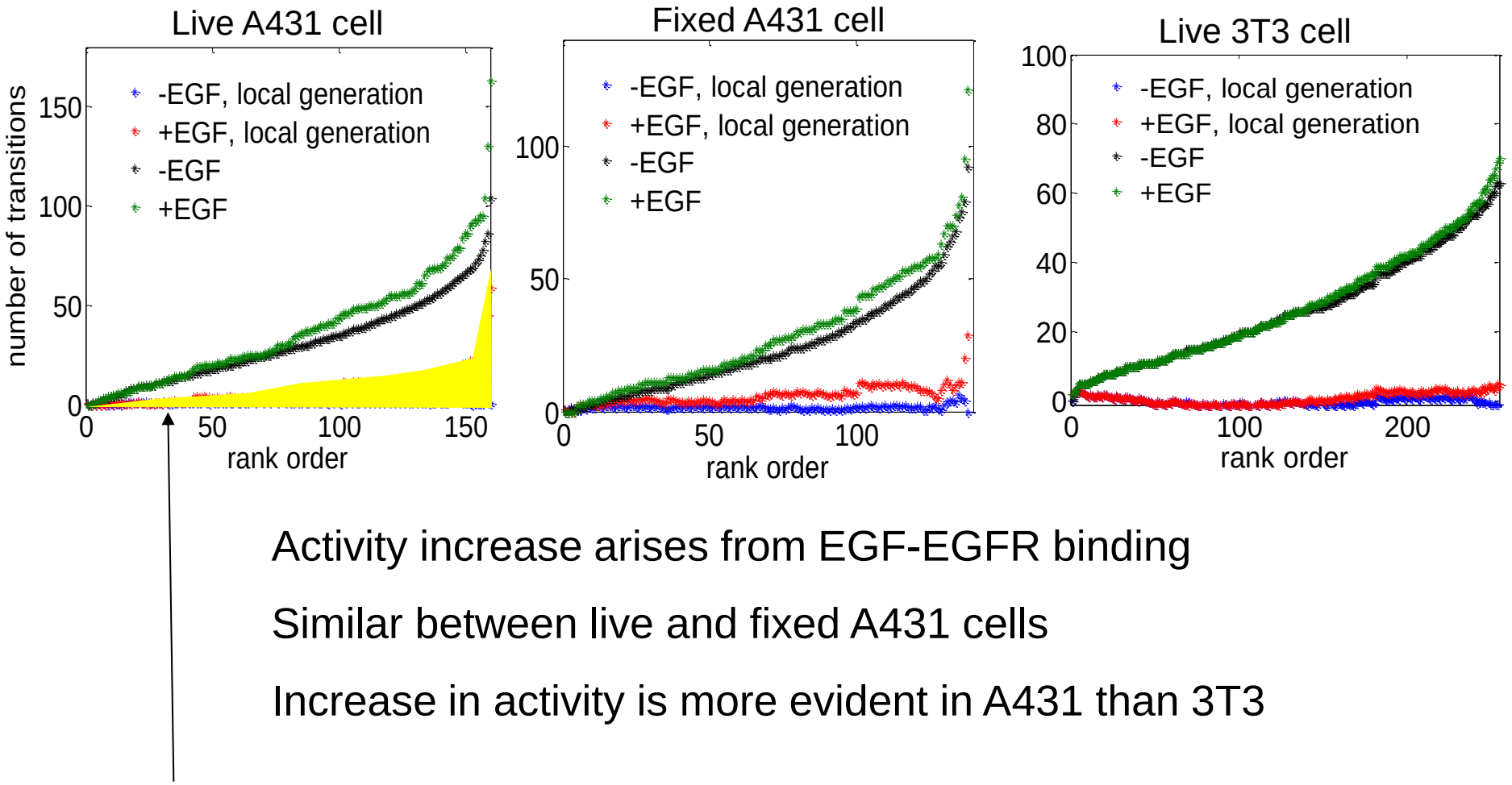

Activity increase arises from EGF-EGFR binding

Similar between live and fixed A431 cells

Increase in activity is more evident in A431 than 3T3

Receptor activity:

SWNT arrays measure receptor activity in real time on a single cell!

Jin, H., et al, Nature Nanotechnology (2010)

Singlet Oxygen ($^1O_2$) Oxidation is the H_2O_2 Source

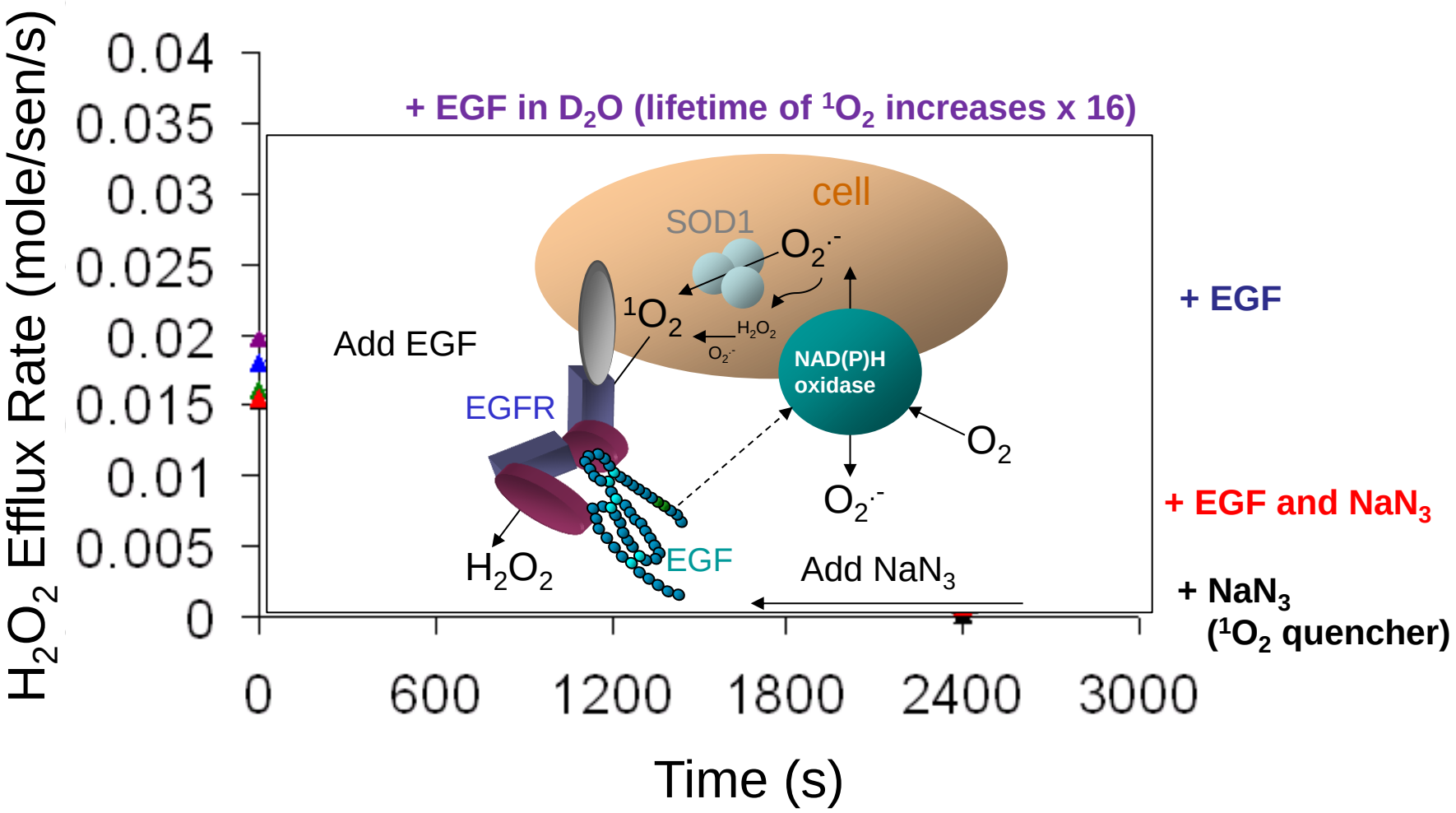

Generation on receptor

$$2^1O_2 + 2H_2O \xrightleftharpoons{EGF-EGFR} 2H_2O_2 + O_2$$

Jin, H., et al, Nature Nanotechnology (2010)

Acknowledgements

Postdoctoral Associates
Jin-Ho Ahn
Moon-Ho Ham
Jae-Hee Han
Zhong Jin
Jong-Ho Kim
Tom McNicholas
Bin Mu
Qing Hua Wang
Kyungsuk Yum

Graduate Students
Joel Abrahamson
Darin Bellisario
Ardemis Boghossian
Peter Bojo
Wonjoon Choi
Lee Drahushuk
Andrew Hilmer
Rishabh Jain
Akira Kudo
Sayalee Mahajan
Geraldine Paulus
Nigel Reuel
Chih-Jen Shih
Steven Shimizu
Zachary Ulissi
Jingqing Zhang

Collaborators
Prof. Daniel Blankschtein (Chem. Eng., MIT)
Prof. Jing Kong (EECS, MIT)
Prof. Pablo Jarillo-Herrero (Physics, MIT)
Prof. Tomas Palacios (EECS, MIT)
Prof. Mildred Dresselhaus (Physics, EECS, MIT)
Prof. A. Castro-Neto (Physics, BU)